**UNIVERSIDADE FEDERAL DO CEARÁ**
**CENTRO DE TECNOLOGIA**
**DEPARTAMENTO DE ENGENHARIA HIDRÁULICA E AMBIENTAL**
**PROGRAMA DE PÓS-GRADUAÇÃO EM ENGENHARIA CIVIL**

**ÁLYSON BRAYNER SOUSA ESTÁCIO**

# CLIMATE CHANGE AND MODEL PARAMETER UNCERTAINTIES PROPAGATED TO UNGAUGED RESERVOIR CATCHMENTS IN CEARÁ: A STUDY FOR WATER AVAILABILITY ASSESSMENT

**FORTALEZA**
**2020**

ÁLYSON BRAYNER SOUSA ESTÁCIO

# CLIMATE CHANGE AND MODEL PARAMETER UNCERTAINTIES PROPAGATED TO UNGAUGED RESERVOIR CATCHMENTS IN CEARÁ: A STUDY FOR WATER AVAILABILITY ASSESSMENT

Dissertação apresentada ao Programa de Pós-Graduação em Engenharia Civil da Universidade Federal do Ceará, como requisito parcial à obtenção do título de Mestre em Engenharia Civil. Área de concentração: Recursos Hídricos.

Orientador: Prof. Dr. Francisco de Assis de Souza Filho.

FORTALEZA
2020

Dados Internacionais de Catalogação na Publicação
Universidade Federal do Ceará
Biblioteca Universitária
Gerada automaticamente pelo módulo Catalog, mediante os dados fornecidos pelo(a) autor(a)

---

E1c Estácio, Ályson Brayner Sousa.
Climate change and model parameter uncertainties propagated to ungauged reservoir catchments in Ceará : A study for water availability assessment / Ályson Brayner Sousa Estácio. – 2020.
67 f. : il. color.

Dissertação (mestrado) – Universidade Federal do Ceará, Centro de Tecnologia, Programa de Pós-Graduação em Engenharia Civil: Recursos Hídricos, Fortaleza, 2020.
Orientação: Prof. Dr. Francisco de Assis de Souza Filho.

1. Incerteza paramétrica. 2. Mudança climática. 3. Regionalização. 4. Disponibilidade hídrica. 5. Modelo conceitual concentrado. I. Título.

CDD 627

---

ÁLYSON BRAYNER SOUSA ESTÁCIO

# CLIMATE CHANGE AND MODEL PARAMETER UNCERTAINTIES PROPAGATED TO UNGAUGED RESERVOIR CATCHMENTS IN CEARÁ: A STUDY FOR WATER AVAILABILITY ASSESSMENT

Dissertação apresentada ao Programa de Pós-Graduação em Engenharia Civil da Universidade Federal do Ceará, como requisito parcial à obtenção do título de Mestre em Engenharia Civil. Área de concentração: Recursos Hídricos.

Aprovado em: 12/02/2020.

BANCA EXAMINADORA

_____
Prof. Dr. Francisco de Assis de Souza Filho (Orientador)
Universidade Federal do Ceará (UFC)

_____
Prof. Dr. Iran Eduardo Lima Neto
Universidade Federal do Ceará (UFC)

_____
Prof. Dr. Eduardo Sávio Passos Rodrigues Martins
Presidente da Fundação Cearense de Meteorologia e Recursos Hídricos (FUNCEME)
Universidade Federal do Ceará (UFC)

_____
Dr. Denis Araujo Mariano
Fundação Cearense de Meteorologia e Recursos Hídricos (FUNCEME)

## ACKNOWLEDGEMENTS

I would like to acknowledge Professor Assis, the Grupo de Gerenciamento de Risco Climático and all those that supported me during the last few months, my fiancée, my parents, sister and friends. No written words are enough to acknowledge them.

This study was financed in part by the Coordenação de Aperfeiçoamento de Pessoal de Nível Superior – Brasil (CAPES) – Finance Code 88887.115878/2015-01; and the Conselho Nacional de Desenvolvimento Científico e Tecnológico (CNPq) – Finance Code 130509/2019-1.

## RESUMO

As mudanças climáticas deverão ter graves consequências sociais e econômicas. No entanto, poucos estudos têm avaliado o impacto das incertezas da mudança climática na disponibilidade hídrica de complexos sistemas de redes de reservatórios. A incerteza é agravada quando os reservatórios não possuem monitoramento das vazões afluentes. Nesses casos, a regionalização dos parâmetros de modelos hidrológicos representa uma estratégia comum para se estimar as vazões afluentes. Propagar as incertezas associadas aos parâmetros para as bacias não monitoradas apresenta-se, no entanto, como um desafio metodológico ainda em discussão. Neste estudo, propõe-se uma estratégia de regionalização, baseada no método de classificação K-Nearest-Neighbor (K-N-N), que incorpora explicitamente as incertezas associadas aos parâmetros do modelo hidrológico. Tais incertezas, bem como aquelas provenientes da mudança climática, foram propagadas para as bacias não monitoradas dos reservatórios no estado do Ceará, tendo sido avaliada a disponibilidade hídrica do Hidrossistema Jaguaribe-Metropolitano. Oito Modelos de Circulação Global (GCMs) da sexta fase do Coupled Model Intercomparison Project (CMIP6) foram usados para representar o clima futuro. A regionalização permitiu cálculo de vazões com *NSE* de 0.67 quando apenas uma bacia preditora é utilizada. Metade dos GCMs projetam um significativo aumento da disponibilidade hídrica no hidrossistema para o período 2021-2050, enquanto que a outra metade prevê diminuição ou manutenção. A incerteza dos parâmetros mostrou-se irrelevante frente a incerteza da mudança do clima. A metodologia proposta deve colaborar com a quantificação das incertezas no Ceará, servindo de ferramenta para o planejamento e gestão dos recursos hídricos locais.



**Palavras-chave**: Incerteza paramétrica. Mudança climática. Regionalização. Disponibilidade hídrica. Modelo conceitual concentrado.

## ABSTRACT

Climate change is expected to have extensive socioeconomic consequences. However, only a few studies have assessed the impact of future streamflow modelling uncertainties in water availability of complex reservoir network systems. This issue is aggravated when the reservoirs do not have inflow measurement. In these cases, regionalizing the hydrological model parameters is a common approach to streamflow estimation. However, propagating these uncertainties to ungauged catchments figures as a methodological question that remains unsolved. In this study we propose a regionalization procedure based on K-Nearest-Neighbor (K-N-N) classification method, that allows to incorporate explicitly the model parameter uncertainty. Climate change and model parameter uncertainties were propagated to ungauged reservoir catchments in Ceará and the future water availability of the Jaguaribe Metropolitan hydrossystem was assessed. Eight Global Circulation Models (GCMs) from the sixth phase of the Coupled Model Intercomparison Project (CMIP6) were used to represent future climate. The K-Nearest-Neighbours regionalization produced accurate streamflow prediction with an average NSE of 0.67, when only the first neighbour is used. Half of GCMs forecasted a significant increase of water availability for the period 2021-2050 in the hydrosystem, while the other half forecasted decrease or maintenance. Parameter uncertainty showed to be negligible in comparison to climate change uncertainty. The proposed framework is expected to collaborate with uncertainty assessment in Ceará, as a tool for water resources planning and management.



**Keywords**: Parameter uncertainty. Climate change. Regionalization. Water availability. Conceptual hydrological model.

## LIST OF FIGURES

## LIST OF TABLES

**TABLE OF CONTENTS**

# 1 INTRODUCTION

Hydrological modelling uncertainties have been subject of interest of the scientific community on the last decades (LIU; GUPTA, 2007; MCMILLAN *et al*., 2011; TUNG, 2018; VALLAM; QIN; YU, 2014). In fact, natural processes randomness makes difficult to predict real systems responses. This randomness results in a natural uncertainty. Additionally, human inability to precisely access information emergent from nature produces an epistemic (or informational) uncertainty (TUNG, 2018).

Epistemic uncertainty appears in hydrological modelling in three categories: input, model structure and parameter uncertainties (GUPTA; GOVINDARAJU, 2019). Input uncertainty is present, for instance, in precipitation and streamflow observed data, resulting from instrument inaccuracies. Additionally, the hydrological model itself is an uncertainty source, since it simplifies the natural system, most of the time using deterministic equations to mimic it. Then, the distance between model and reality and the inability of the former to explain the latter in its complexity result in structural uncertainty. Model parameter identification is a third source of epistemic uncertainty. In fact, different parameter sets may result in an equivalent goodness-of-fit of model response to observed data, that is what Beven and Binley (1992) called equifinality.

The uncertainties present in hydrological data and those added by modelling are propagated along the process of hydrological information production and have impact in water resources planning and management, whose decisions are based in this information (SORDO-WARD *et al*., 2016).

In order to reduce these uncertainties, either by using sophisticated methods for measurement, or model calibration, or by improving the hydrological model, it is necessary not only to identify and understand the uncertainties, but also to quantify them. This quantification allows to assess hydrological information reliability, subsidizing decision making, and also to identify the uncertainties sources more sensitive, promoting an efficient uncertainty reduction (LIU; GUPTA, 2007).

Climate change represent an uncertainty source that may impact society activities on the next decades. This natural and anthropic uncertainty can be assessed by Global Circulation Models (GCMs) projections for different emission scenarios. The Coupled Model Intercomparison Project (CMIP) brings together many GCMs data, which are valuable to climate change uncertainties quantification (GONDIM *et al.*, 2018).

In addition, the development of Monte Carlo Markov Chain (MCMC) samplers

meant advances in uncertainty quantification by Bayesian inference. This approach is mainly used for parameter uncertainty quantification (ENGELAND *et al.*, 2016; GUPTA; GOVINDARAJU, 2019; LIU *et al.*, 2017).

In the State of Ceará, where the water is stored in complex reservoir networks under high hydroclimate variability, the assessment of these uncertainties and their impact on the water resources management have a practical relevance (LIMA NETO; WIEGAND; CARLOS DE ARAÚJO, 2011; MAMEDE *et al.*, 2012). The inflow data scarcity of the most relevant reservoirs generates the need of predicting in ungauged basins by a regionalization framework, which allow to transfer information from one or more gauged catchments to the ungauged ones. This regionalization should also propagate the involved hydrological uncertainties.

In this study, a regionalization procedure is proposed to propagate parameter uncertainty to reservoir catchments in Ceará. The impact of climate change uncertainty on the water availability of the most important hydrosystem in Ceará (i.e. Jaguaribe Metropolitan hydrosystem) was also evaluated and compared to the impact of parameter uncertainty.

## 1.1 Objectives

The main goal of this study was to assess the climate change and parameter uncertainties propagated to the ungauged reservoir catchments in Ceará, evaluating their impacts on the water availability of the Jaguaribe Metropolitan hydrosystem.

For this task, some specific goals were designed:

a) Developing an approach for hydrological model parameter regionalization that is capable to predict the inflow for the reservoirs in the State of Ceará, under parameter uncertainty;
b) Evaluating the adequate number of donor catchments in the regionalization approach to predict model parameters in ungauged catchments in Ceará;
c) Assessing climate change impacts on the future water availability of Jaguaribe Metropolitan hydrosystem, according to CMIP6 GCMs; and
d) Comparing climate change and parameter uncertainties in the Jaguaribe Metropolitan hydrosystem water availability assessment.

## 1.2 Dissertation structure

Following the recent trends in the Departamento de Engenharia Hidráulica e Ambiental of the Universidade Federal do Ceará, this dissertation was structured based on scientific articles. Thus, two articles composed the main chapters of this dissertation, as follow:

a) A K-Nearest-Neighbor regionalization approach to propagate model parameter uncertainty to ungauged catchments; and
b) Assessment of a hydrosystem water availability: a comparison between parameter and climate change uncertainties, using CMIP6 models.

Internal structure of these chapters followed the traditional structure of the scientific articles. A closing section summarized briefly the main conclusions of both researches. References of both articles are presented together in the end of the dissertation.

# 2 FIRST ARTICLE

## A K-Nearest-Neighbor regionalization approach to propagate model parameter uncertainty to ungauged catchments.

**Abstract**:
Regionalizing hydrological model parameters is a common approach to streamflow estimation in ungauged catchments. However, parameter identification in gauged catchments is subject to uncertainty, which is propagated in regionalization. In this study, we propose a regionalization procedure based on the K-Nearest-Neighbour (K-N-N) classification method, that allows to incorporate explicitly model parameter uncertainty. The Differential Evolution Adaptive Metropolis (DREAM) was applied to a conceptual, lumped model calibration and uncertainty assessment. Six physiographic characteristics were assumed for catchment similarity in parameter regionalization. We tried one (1-N-N), three (3-N-N), and five (5-N-N) nearest donor catchments in K-N-N regionalization, which was cross-validated within 28 streamgauges data set. Regionalization produced accurate streamflow series prediction (NSE>0.55). Frequently, 1-N-N approach (NSE=0.67) was a parameter predictor better than 3-N-N (NSE=0.62) or 5-N-N (NSE=0.55). The proposed framework showed to be a valuable tool for water resources management, besides it can be replicated in different hydrological model parameter regionalization.

Keywords: Regionalization. K-Nearest-Neighbour. Conceptual hydrological model. Parameter uncertainty. Bayesian inference.

## 2.1 Introduction

Rainfall-runoff modelling is an essential tool for water resources management (KURTZ et al., 2017; RIVAS-TABARES et al., 2019). Basically, this kind of hydrological model simulates the streamflow produced in a catchment driven by the local climatic conditions. Such approach allows hydrologists to fill gaps in streamflow series and to predict streamflow under different climate scenarios, for example. Water resources managers use this modelling-based information to estimate the water availability and to assess the water security (TRINH *et al.*, 2016; LAFONTAINE *et al.*, 2019).

Model complexity depends on its structure, which can physically represent the hydrological processes in different time scales or only a simple abstraction of them, as in the conceptual models. The model spatial discretization is also an issue. For instance, distributed models divide the catchment area in several cells or in sub-catchments and consider different land properties, while lumped models assume the entire catchment as a uniform unit, disregarding the catchment spatial variability. However, many studies have shown that more complexity in hydrological modelling does not imply better performance (JAKEMAN; HORNBERGER, 1993; ULIANA *et al.*, 2019; VANSTEENKISTE *et al.*, 2014). Actually, conceptual lumped models (CLMs) have been widely used in scientific and practical applications, since they are less demanding in data and computational processing than processes-oriented distributed ones, besides the former can provide a similar performance for the same goals (BENNETT *et al.*, 2016; PONCELET *et al.*, 2017; SEZEN *et al.*, 2019).

In CLMs, the model parameters are the major control of the rainfall-runoff transformation. These parameters implicitly represent the average physiographic characteristics across the catchment. Even if the parameters are related to the physics of the catchment, they cannot be measured in the field. So, in order to determine them, a calibration procedure should be carried out, which allows finding the parameters set that best fits the model response to the observed streamflow.

Although a manual calibration of CLMs can produce sound results, it demands more hydrological expertise, normally does not deal with parameter uncertainty and can be very exhaustive. Therefore, automatic model calibration became a common procedure in hydrology (BARROS, 2007; GAO *et al.*, 2019; NDIRITU; DANIELL, 2001; SHAHED BEHROUZ *et al.*, 2020; ZAKERMOSHFEGH; NEYSHABOURI; LUCAS, 2008). In this context, many optimization algorithms based on heuristics have been developed on the last decades, such as the Particle Swarm Optimization (PSO) (KENNEDY; EBERHART, 2001), the Shuffled

Complex Evolution (SCE-UA) (DUAN; SOROOSHIAN; GUPTA, 1992) and the Evolutionary Algorithms (FOGEL, 1997).

However, either using a manual or an automatic calibration, no set of parameters will give a perfect prediction for streamflow. Many sets of parameters can be considered equally good, depending on which metric is used for testing the model goodness-of-fit. Beven and Binley (1992) called this uncertainty in parameter identification as equifinality, which more recently Smith (2014) named non-identifiability.

Two main approaches can incorporate the parametric uncertainty in model calibration: a multi-objective (or multi-criteria) optimization and the Bayesian algorithms. A multi-criteria calibration considers more than one measure of goodness-of-fit. Each one evaluates one aspect of the streamflow series, either the peaks, the recession or the mean flow. For this approach, in a feasible set of parameters, some solutions can be considered dominated by the others. A parameter solution is dominated by another one, when the latter provides a better model performance, according to all selected criteria. The non-dominated solutions, in turn, are those that present a trade-off of performance, making impossible to choose a better solution among them. The non-dominated parameter values form a set of best solutions, called Pareto front. In this regard, multi-criteria versions of heuristic algorithms began to be developed, such as the Multi-objective Particle Swarm Optimization – MOPSO (COELLO; LECHUGA, 2002) and the Multi-objective Shuffled Complex Evolution - MOSCEM Metropolis (VRUGT *et al.*, 2003), which has been widely applied for model calibration and equifinality assessment (BARROS *et al.*, 2010; HERNANDEZ-SUAREZ *et al.*, 2018; KAMALI; MOUSAVI; ABBASPOUR, 2013).

In the Bayesian inference, the model parameters are considered as random variables, whose distributions can be gradually approached by observed data assimilation. In this way, Beven and Binley (1992) proposed the Generalized Likelihood Uncertainty Estimation (GLUE), which uses maximum likelihood estimators to find out the parameter distribution. Afterwards, Vrugt *et al.* (2008) developed the Differential Evolution Adaptive Metropolis (DREAM), a Markov Chain Monte Carlo (MCMC) sampler that provides a fast convergence in Bayesian inference, which showed to be a very useful tool for hydrological model calibration under uncertainty (ASFAW; SHUCKSMITH; MACDONALD, 2016; RWASOKA *et al.*, 2014; SHAFII; TOLSON; MATOTT, 2014).

However, the most of rainfall-runoff model applications has been carried out for ungauged catchments, where streamflow data do not exist or are very scarce. Because of its important role in real-world problems, predicting in ungauged basins (PUB) has been

recognized as one of the main scientific frontiers in hydrological sciences (WAGENER; MONTANARI, 2011) and was targeted as a major scientific initiative of the past decade by the International Association of Hydrological Sciences (IAHS) (SIVAPALAN *et al.*, 2003).

Basically, PUB normally involves applying regionalization techniques, which transfer hydrological models and parameters calibrated from a set of donor gauged basins, in order to predict hydrological dynamics and/or statistics for ungauged systems. Three approaches are normally used for transferring calibrated parameters: regression (parameter estimation from relations to catchment physical and climatic characteristics), nearest neighbours (parameter transfer from catchments similar in attribute space) and geostatistics (parameter spatial interpolation) (e.g. MERZ AND BLÖSCHL 2004, VIVIROLI *et al.* 2009, SAMUEL *et al.* 2011, WALLNER *et al.* 2013).

In the State of Ceará located in the semi-arid northeast of Brazil, many surface reservoirs have been built, to overcome dry seasons and recurrent pluriannual droughts that have induced serious social impacts and economic losses in the last century. In Ceará, there are more than 25,000 reservoirs (>0.5 $hm^3$) (CAMPOS *et al.*, 2016), with 155 of them being operated by government agencies. These regulated reservoirs store about 18.6 billion $m^3$, which supports the greater part of the state water supply (>90%) (SOUZA FILHO, 2018).

Despite their very important role on the water availability, those reservoirs do not have inflow measurement. For this reason, practitioners have estimated the inflow series to the reservoirs assuming the discharge from the nearest upstream streamgauge, with simple water balance for streamflow propagation. However, there are two main limitations for this approach. First, the rainfall-runoff processes of the ungauged area are not taken into account. Second, the modelling uncertainty is neglected. Thus, hydrological model regionalization is needed for the reservoirs in the State of Ceará.

The goal of this work is to develop a streamflow regionalization approach that is capable to predict the inflow and its associated parameter uncertainties for the reservoirs in the State of Ceará, NE Brazil. We use DREAM to calibrate a conceptual lumped rainfall-runoff model and to assess the model parameter uncertainty. Then, we propose a K-Nearest-Neighbours (K-N-N) regionalization approach for the calibrated parameters, which allows the propagation of parameter uncertainty to ungauged catchments, considering six physiographic characteristics. To evaluate the regionalization performance, cross-validation of gauged catchments is applied.

## 2.2 Study area hydro-climatology

The State of Ceará (148,000 km$^2$) has about 90% of its territory in a semi-arid region, called Polygon of Droughts. Mean annual rainfall is about 800 mm, ranging from more than 1,200 mm close to the coast to less than 650 mm in a large dryland landscape that extends from the coast to the interior borders (SOUZA FILHO, 2018). Rainfall is concentrated mainly within the rainy season, which normally lasts four months (February-May). Interannual rainfall variability is high with a coefficient of variation (CV) of 0.36 (GÜNTNER; BRONSTERT, 2004). Temporal variability is also highly significant on seasonal and weekly scales. The annual potential evaporation (class A pan) of the semiarid region is about 2,200 mm (SUDENE 1980).

Groundwater resources are scarce and concentrated. They occur mainly in sedimentary rocks: the interior Iguatu Basin, the Araripe/Cariri Basin in the very south, the Apodi Plateau in the east, the Ibiapaba Plateau in the west and the sedimentary rocks on the coast (FRISCHKORN; SANTIAGO; DE ARAUJO, 2003). Local alluvial aquifers in riverscapes are well spread over the state and embedded in crystalline bedrocks with a low density of fractures (FRISCHKORN; SANTIAGO; DE ARAUJO, 2003).

About 80% of the study area is characterized by crystalline bedrock and shallow soils. A xerophytic thorn-bearing woodland, mainly deciduous in the dry seasons, is the dominant natural vegetation type: the Brazilian dry forest called *Caatinga*. Real evapotranspiration is about 78% of annual rainfall, with percolation to the underlying groundwater or bedrock system 9% and runoff 13% on average (SUDENE, 1980). Mean annual flow of large rivers ranges from 10 to 20% of annual rainfall and the respective CV is generally above 1.0 (GÜNTNER; BRONSTERT, 2004). It is expected that the large rivers are dominantly endogenous throughout the rainy seasons and interact with the underlying groundwater, mainly by groundwater recharge (based on COSTA *et al.* 2012, 2013).

## 2.3 Climate and hydrology data

We selected twenty-eight streamgauges from the Brazilian Water Agency (ANA) as streamflow database to calibrate and validate the rainfall-runoff model. The drainage area of selected stations varies from 46 km² to 48,000 km² (Figure 1). Only the streamgauges with monthly data series with duration equal to or longer than 10 years were chosen. These gauges are well distributed over the state and their catchments cover most of it.

Figure 1 – The twenty-eight selected streamgauges in the state of Ceará, NE Brazil.

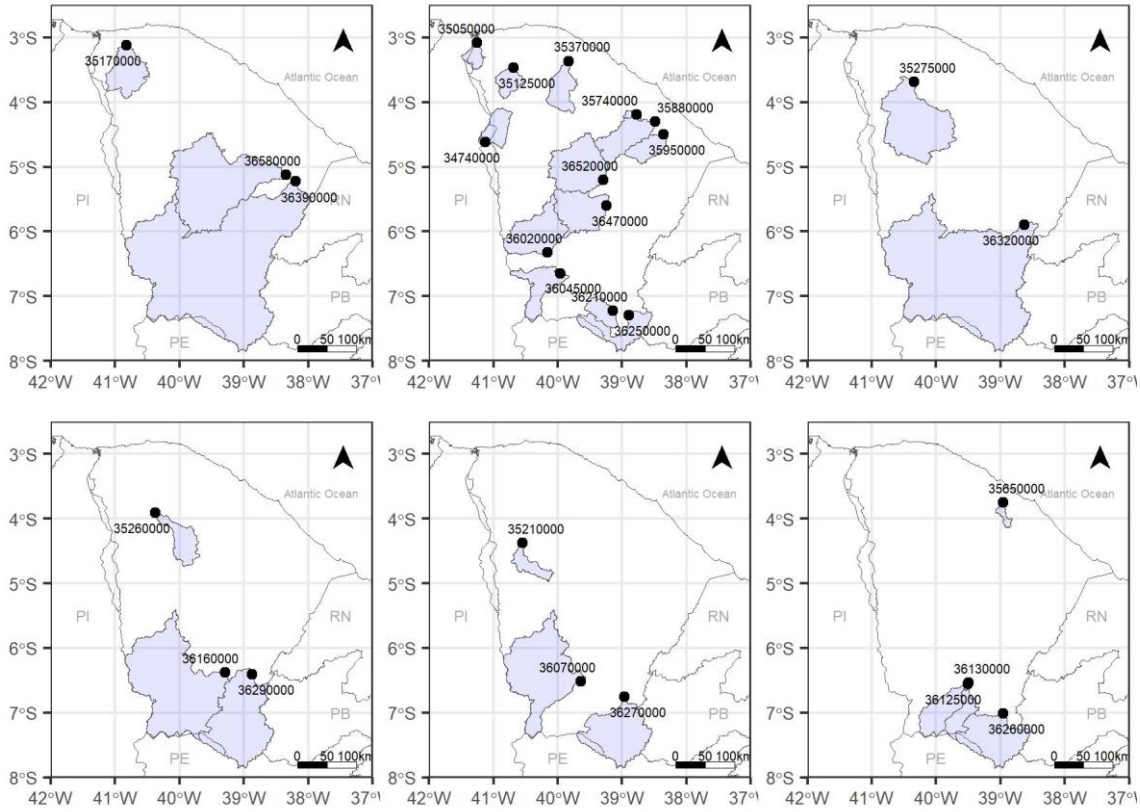


Source: Elaborated by the author.

Monthly rainfall time series of the streamgauge catchments were based on 815 rain gauges data from different state-based and national Institutes, which were made available by ANA. The inverse distance weighting was used as interpolation approach, which allowed considering a smooth precipitation variation between the rain gauges and to estimate the precipitation in locations with no available data (PLOUFFE; ROBERTSON; CHANDRAPALA, 2015). The period of the rainfall series was from 1910 to 2017.

Daily meteorological data (air temperature, air humidity and short-wave radiation) were made available by the Brazilian Institute of Meteorology (INMET), to calculate potential evapotranspiration with the Penman-Monteith equation. The monthly evapotranspiration time series of the streamgauge catchments were derived using the Thiessen polygons.

## 2.4 Methods

The proposed framework (Figure 2) allows to predict streamflow in ungauged catchments, using a K-N-N regionalization approach that transfers rainfall-runoff model parameters from donor catchments to the targeted ones. In this regionalization, a similarity

assessment between donor and targeted catchments was driven by six catchment physiographic characteristics. A multiple linear regression model was used to obtain the weighting coefficient of each characteristic, providing, in this way, the relevance of that characteristic for streamflow prediction.

The developed approach differs from the traditional regionalization, because it propagates rainfall-runoff model parameter uncertainty to ungauged catchments. The DREAM algorithm was used to calculate the parameter distributions from the donor catchments. The rainfall-runoff model selected was Soil Moisture Accounting Procedure (SMAP), a conceptual lumped model, which have been frequently applied for water resources assessment in Ceara drylands (FERNANDES et al., 2017; SILVEIRA; SOUZA FILHO; VASCONCELOS JÚNIOR, 2017).

Figure 2 – Proposed framework for streamflow prediction to ungauged catchments under parameter uncertainty, using a K-N-N regionalization approach.

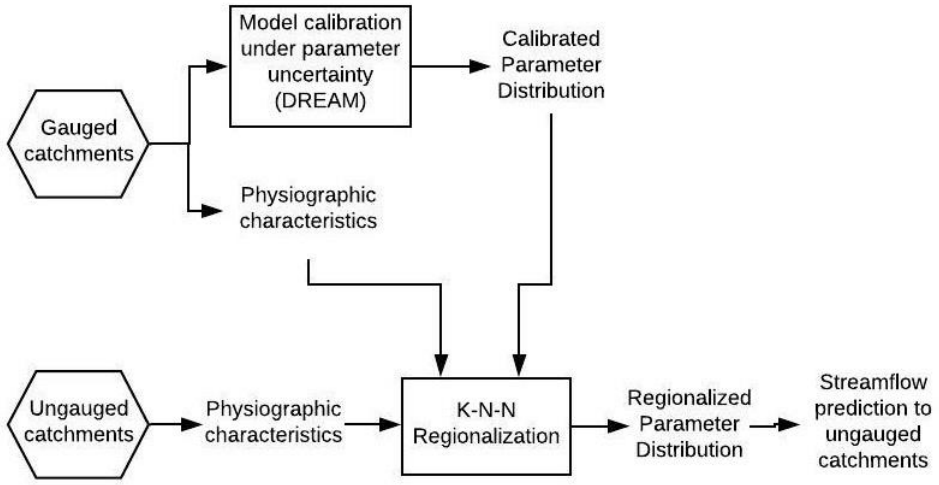


Source: Elaborated by the author.

### *2.4.1 Rainfall-runoff model*

The streamflow generation at catchment scale was simulated by the monthly version of the Soil Moisture Accounting Procedure (SMAP) (FERNANDES et al., 2017; LOPES; BRAGA; CONEJO, 1981; SILVEIRA; SOUZA FILHO; VASCONCELOS JÚNIOR, 2017). Figure 3 provides an overview of the model structure, showing connected reservoirs, inputs, internal water fluxes and outputs. In its monthly version, SMAP has two reservoirs, soil ($R_{soil}$) and underground ($R_{undergr}$), which simply represent the vadose zone and the aquifer, respectively.

Figure 3– Monthly SMAP model structure representation with connected reservoirs, inputs, internal water fluxes and outputs.

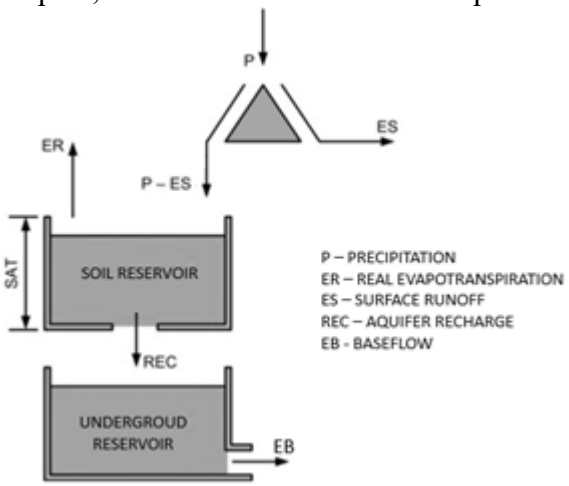


Source: Adapted from Lopes *et al.* 1981.

Applying mass conservation for both reservoirs, the following equations are formulated:

$$\frac{d\,R_{soil}}{dt} = P - Es - Er - REC \tag{1}$$

$$\frac{d\,R_{undergr}}{dt} = REC - Eb \tag{2}$$

Where $P$, $Er$, $Es$, $REC$ and $Eb$ is the precipitation, the real evapotranspiration, the surface runoff (or the fast flow), the aquifer recharge and the baseflow (or the slow flow), respectively.

Real evapotranspiration depends on the potential evapotranspiration ($EP$) and the soil moisture in the vadose zone $\left(\frac{R_{soil}}{SAT}\right)$. This relation is mimicked by equation (3):

$$Er = \left(\frac{R_{soil}}{SAT}\right) EP \tag{3}$$

The average catchment characteristics drive the flux between the reservoirs and their outflow, as follow:

$$Es = P\left(\frac{R_{soil}}{SAT}\right)^{PES} \tag{4}$$

$$Eb = \left[1 - \left(\frac{1}{2}\right)^{\frac{1}{K}}\right] R_{undergr} \tag{5}$$

$$REC = CREC\left(\frac{R_{soil}}{SAT}\right)^{4} R_{soil} \quad (6)$$

Where $SAT$, $PES$, $CREC$ and $K$ are the model parameters that have to be calibrated. These parameters may be related to the catchment physiographic characteristics. $SAT$ represents the maximum depth of the soil reservoir. So, $\frac{R_{soil}}{SAT}$ is the relative soil moisture, which is relevant for the computation of surface runoff (fast flow), aquifer recharge and also real evapotranspiration. $PES$ and $CREC$ are dimensionless coefficients, which are a function of the catchment shape, the relief, the soil texture and permeability, driving the infiltration-runoff partition and the (deep) percolation towards the aquifer. Finally, $K$ controls the aquifer discharge, which generates baseflow (slow flow).

According to Lopes *et al.* (1981) and Alexandre (2005), the four model parameters are limited by the following ranges:

Table 1 - SMAP parameter ranges.

| Parameter | Limit | |
|---|---|---|
| | Inferior | Superior |
| *SAT* | 400 | 5000 |
| *PES* | 0.1 | 10 |
| *CREC* | 0 | 70 |
| *K* | 1 | 6 |

Source: Elaborated by the author.

The initial values of both reservoirs determine the model initialization. Assuming that the local semi-arid aquifers dry out after 6-8 months of dry season, we set the initial underground reservoir value as zero at the beginning of the rainy season. For the soil reservoir, we arbitrarily initialized it as 30% of $SAT$. The effect of the model initialization on the streamflow simulation was minimized by a model warm-up of 12 months, which showed to be enough computation time for the simulation convergence of the monthly SMAP model.

### *2.4.2 Model calibration and validation under parameter uncertainty*

In order to take into account the parameter uncertainty, we used the algorithm DREAM (VRUGT *et al.*, 2008) to calibrate the SMAP parameters. DREAM uses a MCMC sampler, which allows to determine the model parameters under a Bayesian inference approach. In this procedure, the information about the parameter values ($\theta$) and its uncertainty are

provided by probability distributions, while data observation ($D$) in comparison to the model response updates those distributions, as it is summarized in equation (7) (BLITZSTEIN; HWANG, 2019):

$$P(\theta|D) = \frac{P(\theta)P(D|\theta)}{P(D)} \tag{7}$$

Where $P(\theta)$ and $P(\theta|D)$ represent the prior and posterior distribution of $\theta$. $P(D)$ is a scalar and does not depend on $\theta$, so calculating $P(D)$ is irrelevant to $\theta$ updating. $P(D|\theta)$ denotes the probability of obtaining observation $D$ given $\theta$, and it is equivalent to the likelihood function $L(D)$. From $L(D)$ we update the distribution of $\theta$, weighting the sampled values (VRUGT *et al.*, 2008).

We assumed that model errors, which are defined as the difference between the model response and observation, are independent and Gaussian distributed. So, the likelihood function could be calculated as in equation (8) (VRUGT, 2016).

$$L(D) = \prod_{t=1}^{n} \frac{1}{\sqrt{2\pi{\sigma_e}^2}} exp\left[-\frac{1}{2}\left(\frac{e_t}{\sigma_e}\right)^2\right] \tag{8}$$

Where $e_t$ is the model error and $\sigma_e$ is its standard deviation. Due to the model non-linearity, a sampler was required to obtain the $\theta$ posterior distribution. That sampler was provided by DREAM. The MCMC is an algorithm of fast convergence, which determines the posterior distribution of parameters and its uncertainty by the ensemble of chains.

Then, the uncertainty is propagated by simulating rainfall-runoff transformation for each set of parameters from the 100-last elements of the 10-converged chains. The performance of the 1000 streamflow simulated series was evaluated using the Nash-Sutcliffe Efficiency Coefficient ($NSE$) (equation 9), which is considered an adequate goodness-of-fit measure for hydrological model calibration and validation (LIN; CHEN; YAO, 2017).

$$NSE = 1 - \frac{\sum_{t=1}^{n}(Q_{obs_t} - Q_{calc_t})^2}{\sum_{t=1}^{n}(Q_{obs_t} - \overline{Q_{obs}})^2} \tag{9}$$

Where $Q_{obs_t}$ and $Q_{calc_t}$ are the streamflow observations and the model response, respectively, and $\overline{Q_{obs}}$ is the average streamflow observation. $NSE$ varies between 1 and -∞. Hypothetically, it achieves the unity when there is no deviation between observation and the model response, while negative values for $NSE$ indicates that $\overline{Q_{obs}}$ is a better estimation than the model response. Moriasi *et al.* (2007) point out that values of $NSE$ around 0.5 or more are considered satisfactory for hydrological modelling. So, the 1000 streamflow simulated series for each catchment result a set of 1000 $NSE$ values.

To validate the calibration of each streamgauge, we selected 30% of the whole time series, which was not used in calibration, according to the Split-Sample Test (Klemes 1986). Moreover, we included both wet and dry years in the selection, in order to represent fairly the climate regime in calibration and validation.

### *2.4.3 Regionalization procedure*

Since the model parameters may be related to the average characteristics of the catchment, we expect that similar catchments may present similar parameters. Therefore, we selected six physiographic characteristics, which could help estimate the model parameters in ungauged systems.

Characteristics, such as the portion area on the crystalline bedrock and the available water capacity (AWC), may provide information about the storage capacity of the catchment. Since the Curve Number varies accordingly to the soil group and the dominant land use, it may be related to infiltration-runoff relationships, soil moisture and (deep) percolation. Other characteristics, such as the drainage density, the average slope and the compactness coefficient of the catchment, may be connected to the water transport in the catchment. Table 2 summarizes the selected characteristics and their database source, which enabled us to calculate their average values for each streamgauge catchment.

Table 2 - Catchment physiographic characteristics.

| **Characteristic** | **Source** |
|---|---|
| Portion area on crystalline bedrock - Cryst | Regionalized Data (COGERH 2013) |
| Gravelius Compactness Coefficient - Kc | Calculated by the author |
| Drainage density – DD | Regionalized Data (COGERH 2013) |
| Available water capacity– AWC | Regionalized Data (COGERH 2013) |
| Average Catchment Slope - Slope | Brasil em Relevo (MIRANDA, 2005) |
| Runoff Curve Number – CN | GCN250 (JAAFAR; AHMAD, 2019) |

Source: Elaborated by the author.

Those average catchment characteristics were then used for the K-Nearest-Neighbour (K-N-N) regionalization approach, in order to estimate the model parameters for ungauged catchments. K-N-N is a classification method that recognizes the similarity between the elements of a classified group and a new unclassified element. This similarity is based on a measure of distance between the new element and the other ones in a space of chosen characteristics (CUNNINGHAM; DELANY, 2007).

So, the ungauged catchment was related to the more similar gauged catchments, according to their physiographic characteristics. We used the parameter distributions, which were obtained by applying DREAM, from the donor catchments to the targeted one. The Euclidean distance (equation 10) was assumed as similarity measure. Before applying the equation 10, we standardized the characteristic variables, removing their scales and dimensions. Also, as each characteristic has its own relevance to the rainfall-runoff process, we weighted their standardized values after their influence on runoff generation at catchment scale.

We assumed that the most relevant characteristics are more correlated to the long-term streamflow. So, to obtain the weighting coefficients, we fitted a multiple linear regression between the standardized physiographic characteristics and the streamflow in mm/year (SOUZA FILHO; LALL, 2003). We also included annual precipitation (P) as an independent variable, since it is the most relevant driving force of the rainfall-runoff process. This variable was also standardized. Finally, the regression coefficients gave the weights for the K-N-N regionalization.

$$D_{E\,(a,b)} = \sqrt{\sum_{i=1}^{n}\left[w_i(c_{i_a} - c_{i_b})\right]^2} \tag{10}$$

$D_{E\,(a,b)}$ is the Euclidean distance between the catchments $a$ and $b$ in the streamflow space. $c_{i_a}$and $c_{i_b}$represent the standardized physiographic characteristic $i$ of the catchments $a$ and $b$. $w_i$ represent the weight of the characteristic $i$.

We tried one (1-N-N), three (3-N-N), and five (5-N-N) nearest donor catchments. For the 1-N-N approach, the 1000-values set of parameters came directly from the nearest donor catchment, while for the 3-N-N and 5-N-N ones, the 1000 parameters were randomly selected from the three and five nearest donor catchments, respectively. To evaluate the performance of the proposed regionalization, we used a cross-validation approach. We considered each one of the twenty-eight streamgauge catchments as an ungauged one and the rest of them as possible donor catchments. Thus, we first transferred the parameter distributions from the donor catchments to the ungauged ones, after the regionalization procedure, then, we simulated a set of streamflow series for the ungauged catchment. Finally, $NSE$ was calculated to evaluate the regionalization performance.

## 2.5 Results and Discussion

### *2.5.1 Calibrated parameters and semi-arid catchment hydrology*

The 1000-value sets of calibrated parameters were used to establish the posterior parameter distributions, which were assessed using their histograms for each streamgauge (Figure 4a and 4b). In general, DREAM was able to find out 'well-behaved' posterior distributions from priors. $SAT$ and $PES$ parameter sets resulted in bell-shaped histograms, which implied that these parameters were well identifiable. Moreover, sharp $SAT$ and $PES$ distributions indicated low equifinality of these parameters.

$SAT$ values varied from low to intermediate (< 3000 mm), wherein the most of streamgauges (twenty-four out of twenty-eight) presented $SAT$ values lower than 2000 mm. These outcomes are probably related to the dominant presence of shallow soils, rock outcrops and low-capacity of natural and anthropized dry forest. Moreover, most of streamgauges (exactly ¾) had also low to intermediate $PES$ values (< 5), which facilitate runoff generation at infiltration-runoff partition. This finding was expected for the studied catchments, where the fast flow is the main component of the large and medium-sized river streamflow.

The semi-arid river intermittence came from a negligible aquifer storage capacity that produces low baseflow. This natural pattern was mimicked by the low $CREC$ values found in the calibration. Actually, a $CREC$ close to zero means no relevant aquifer recharge is produced and, consequently, no underground reservoir. This result is similar to the outcomes from Alexandre (2005), who found very low *CREC* values for Ceará-based catchments after traditional SMAP calibration approaches.

Moreover, when $CREC$ is (almost) zero, $K$, which drives the underground reservoir storage depletion, is indifferent, because negligible aquifer storage provides no relevant baseflow, whatever its depletion is. Therefore, $K$ could assume any value from its given range. This *CREC* and *K* pattern was found out in twenty-five out of the selected streamgauges (see Figure 5: high *K* standard deviation and high *CREC* skewness), and was depicted in Figures 6a1, 6a2 and 6a3 that show the 36130000, 36125000 and 36270000 streamgauge, respectively.

Figure 4a – Parameter posterior distributions for streamgauges from 34740000 to 36045000.

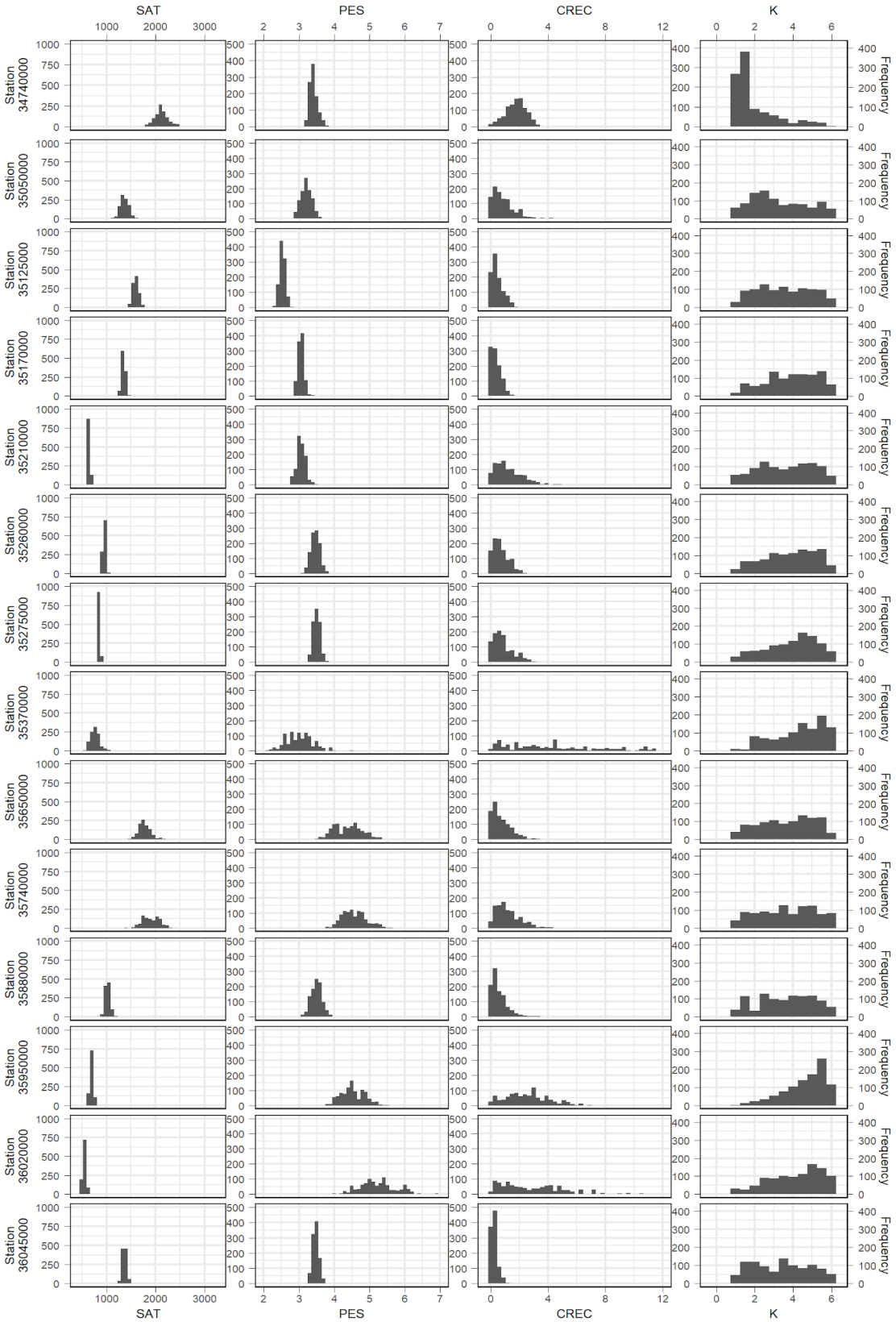


Source: Elaborated by the author.

Figure 4b – Parameter posterior distributions for the streamgauges from 36070000 to 36580000.

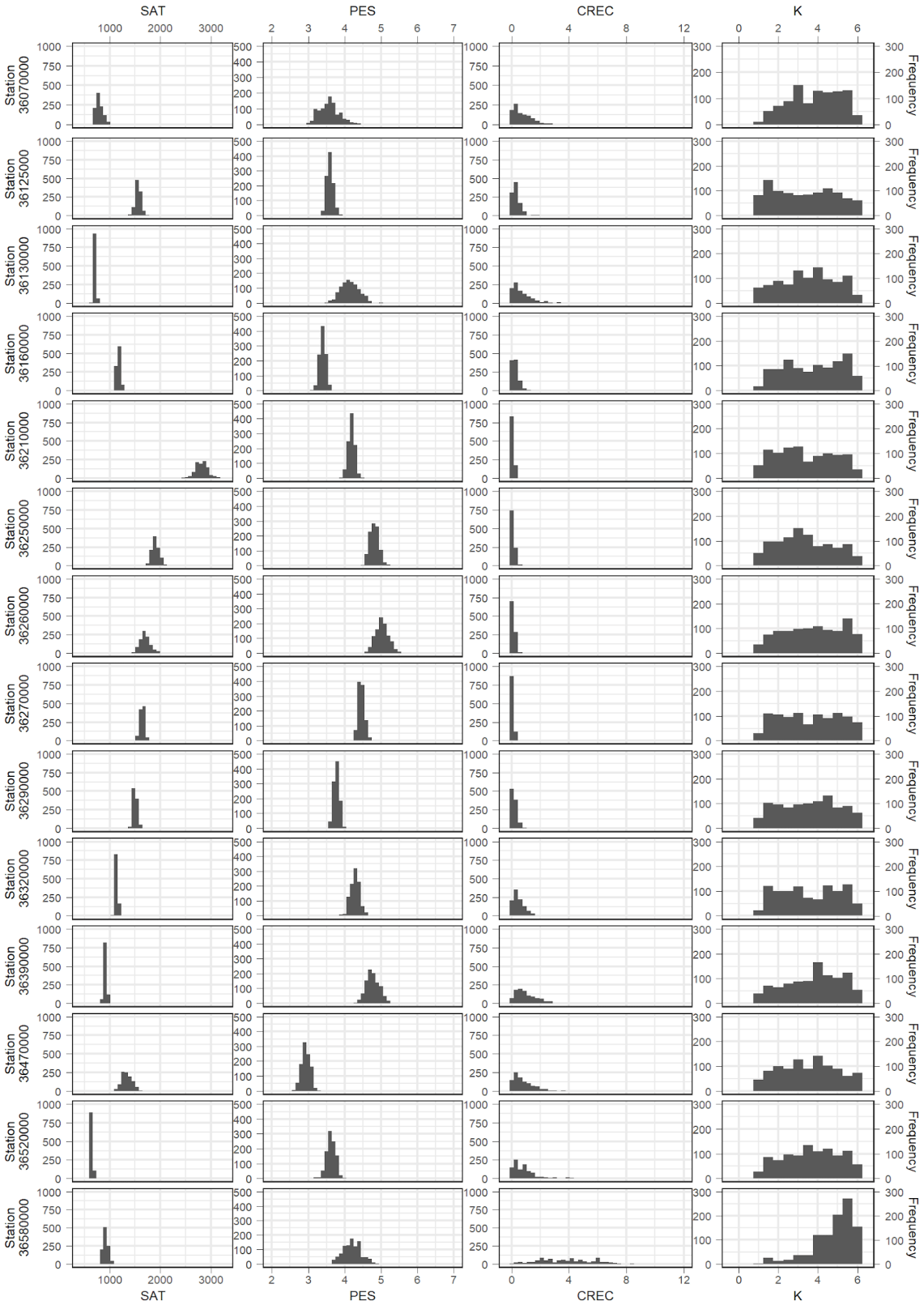


Source: Elaborated by the author.

However, three streamgauges presented a different *CREC* and *K* pattern (see Figure 5), as one can closely observe in Figure 6b1, 6b2 and 6b3. The 34740000 streamgauge (Figure 6b1) is located in the sedimentary Ibiapaba Plateau on the East border of Ceará. Its catchment is the only one that presented zero portion area on the crystalline bedrock, which may indicate a relevant aquifer storage in the sedimentary layers during the wet years. Therefore, this aquifer may sustain the baseflow detected in the 34740000 streamgauge, although the low values of *K* imply a slower groundwater flow response. The 35950000 streamgauge catchment (Figure 6b2) presented a very low average slope (<4%) due to a large portion of lowlands, which can favour the recharge into local aquifers (relevant *CREC* values), draining fast out (higher *K* values) because of dominant intermittent groundwater flow there. The 36580000 streamgauge catchment (Figure 6b3) behaved similarly to the latter one, but no clear reason could be formulated from the average physiographic characteristics of the catchment.

Figure 5 – $CREC$ skewness *vs.* and $K$ standard deviation.

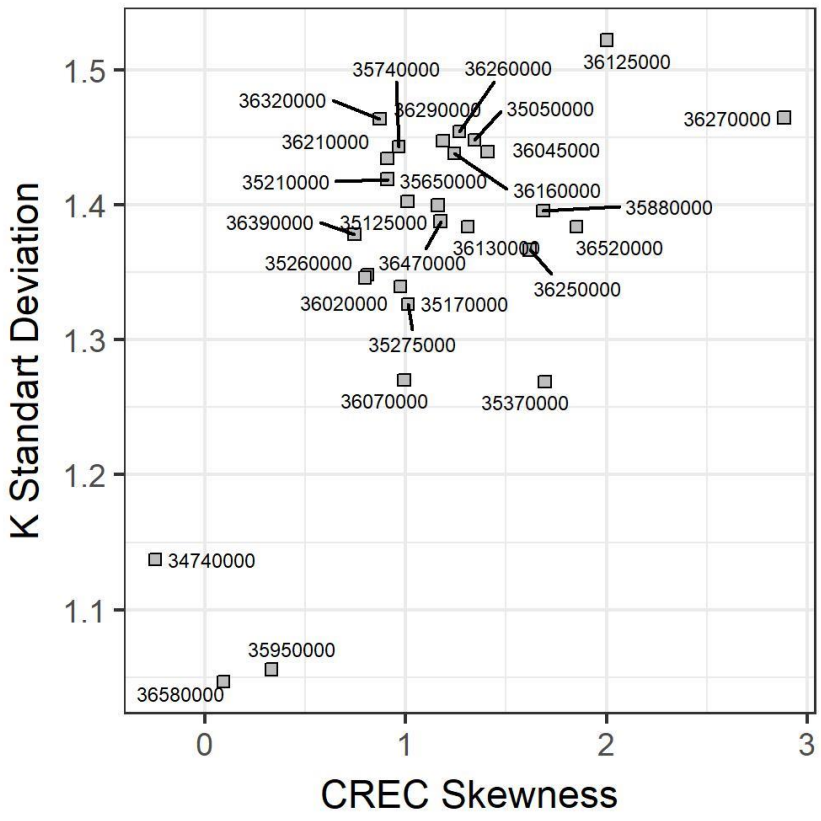


Source: Elaborated by the author.

Figure 6 – The $CREC$ and $K$ posterior distributions for the streamgauges: 36130000 (a1), 36125000 (a2), 36270000 (a3), 34740000 (b1), 35950000 (b2), and 36580000 (b3), where the first three show similar distributions to 25 streamgauges and the last three a particular pattern explained in the text.

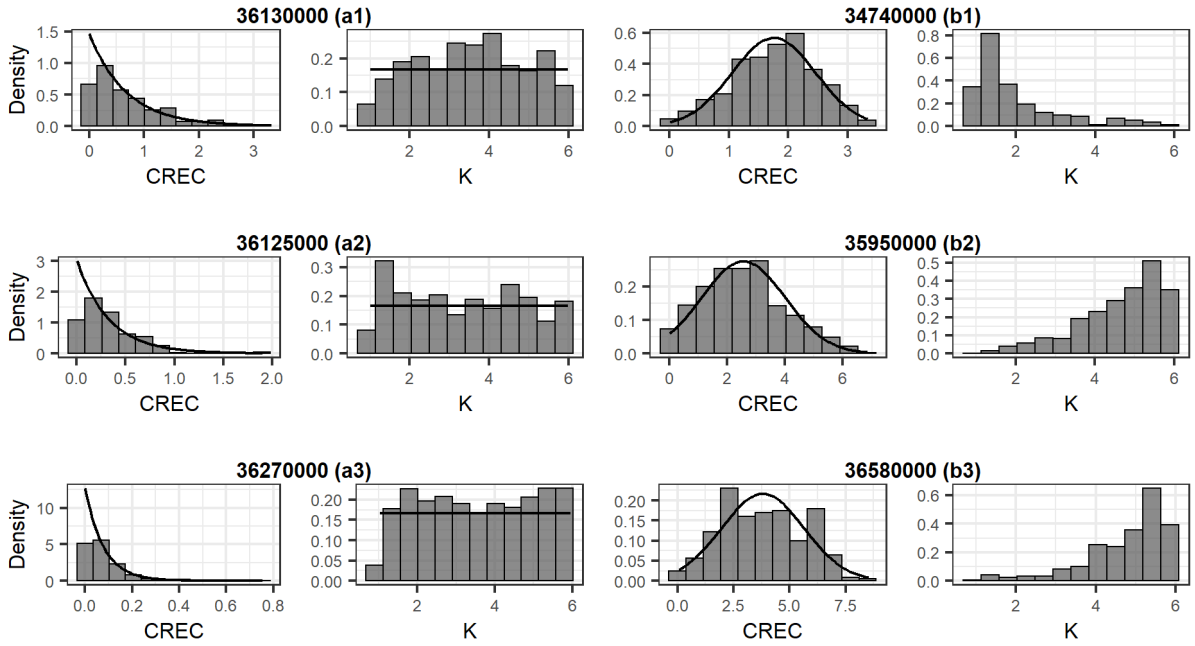


Source: Elaborated by the author.

### *2.5.2 Rainfall-runoff model performance in calibration and validation*

Simulating the rainfall-runoff model using the 1000-value parameter set, we calculated 1000 streamflow series, which represent the involved parametric uncertainty. First, we analysed the model performance visually in calibration and validation. For instance, we plotted the observed and the 1000 simulated streamflow time series for 34740000 and 36260000 streamgauge catchments (Figure 7). We found that the model predicted the recession limb of the hydrographs and the non-flow periods, accurately. In recession, the uncertainty band became larger and often enveloped the observed streamflow. The model also predicted accurately the rising limb of the hydrographs with a narrow uncertainty band. On the other hand, larger errors were observed for streamflow peaks in both calibration and validation. Moreover, the interannual streamflow variability was well fitted by the applied approach, including extreme wet years, (very) sharp streamflow state transition and hydrological droughts.

Figure 7 –Simulated and observed streamflow time series for the 34740000 and 36260000 streamgauges.

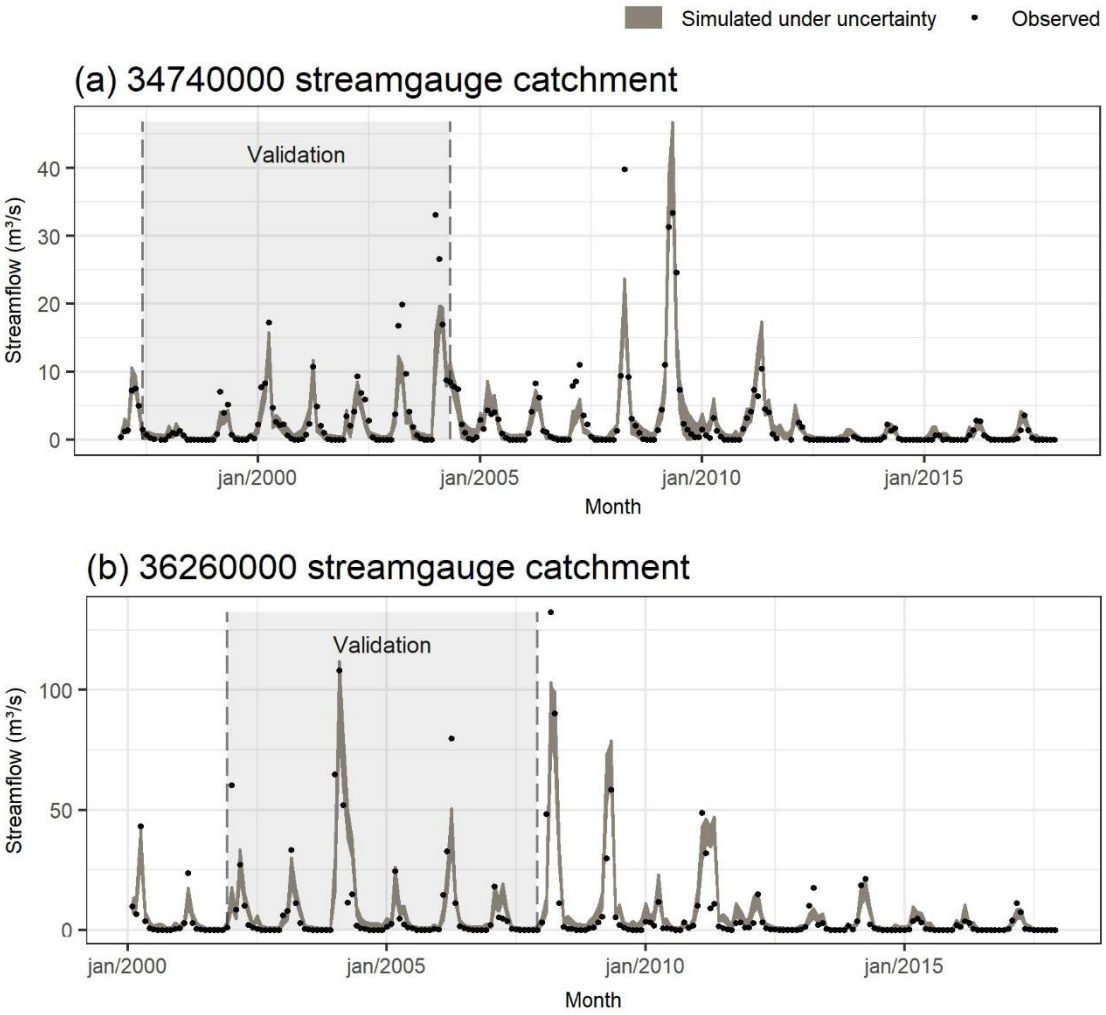


Source: Elaborated by the author.

The evaluation of the 1000-simulated streamflow series provided 1000 $NSE$ values for each streamgauge in calibration and validation. The average and the standard deviation of the $NSE$ sets are presented in Figure 8. In twenty-three out of the twenty-eight evaluated streamgauges, the average $NSE$ evaluated in the calibration period ($NSE_{cal}$) was higher than the average $NSE$ for validation ($NSE_{val}$), as expected. For twenty-six streamgauges, $NSE_{cal}$ and $NSE_{val}$ were higher than 0.5 and for all of them *NSE* were higher than 0.4. Then, the model performance results can be considered satisfactory for monthly dryland streamflow after Moriasi *et al.* (2007). Additionally, we also found that the differences between $NSE_{val}$ and $NSE_{cal}$ standard deviations were negligible (less than 0.100) (Figure 8). Therefore, model performance uncertainty was slightly the same for calibration and validation.

Figure 8 – Average and Standard Deviation of 1000 *NSE* values for each studied streamgauge in calibration and validation. See details in the text.

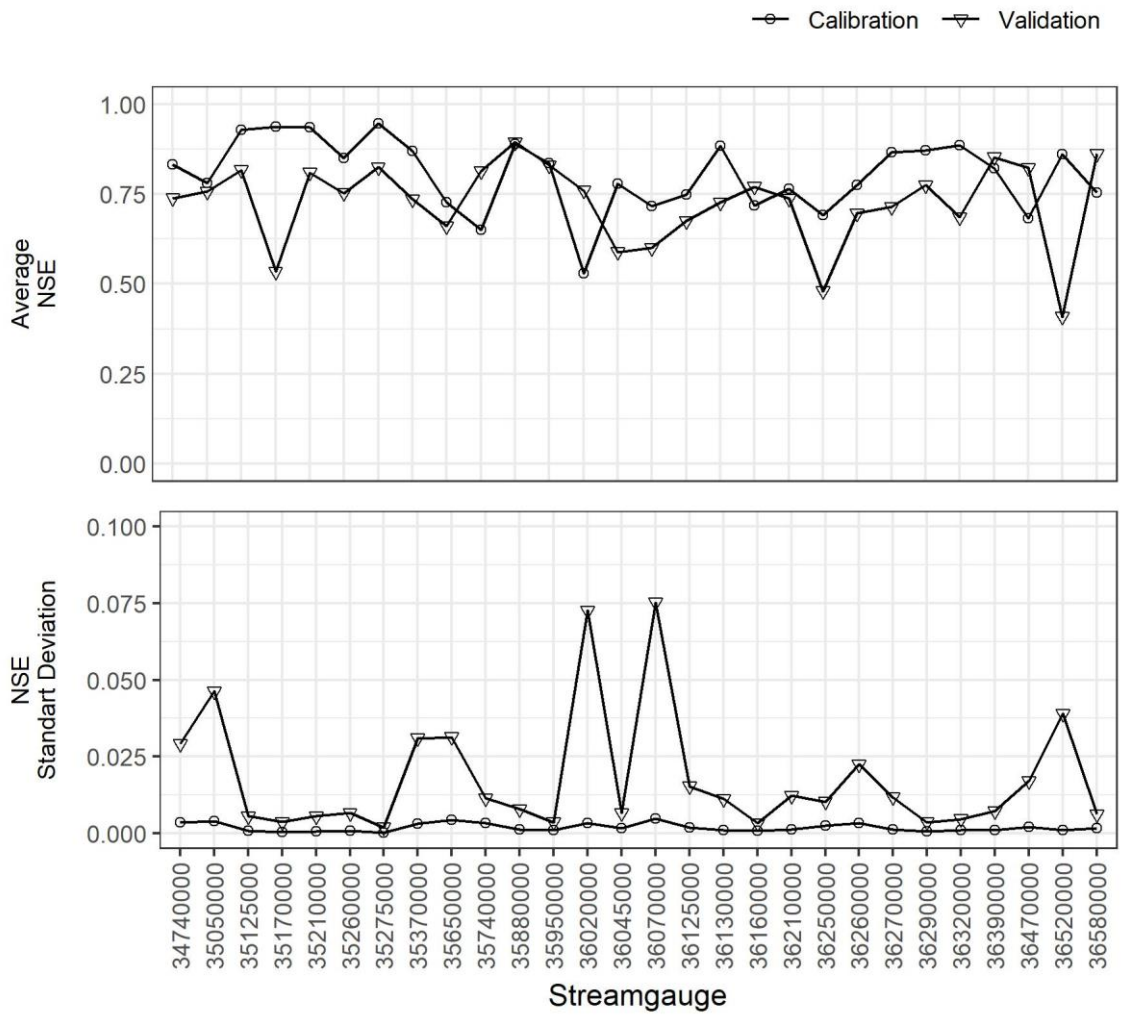


Source: Elaborated by the author.

### *2.5.3 Catchment physiographic characteristics and weighting coefficients*

Table 3 summarizes physiographic characteristics calculated for the selected streamgauge catchments. The average portion area on crystalline bedrock (Cryst) was approximately 80%, with more than ¾ of catchments presenting values superior than 90%. Only one catchment (34740000) was completely located in a sedimentary region. Gravelius Compactness Coefficient (Kc) ranged from 1.8 to 3.2, indicating that the study area catchment shapes are quite irregular. In addition, average drainage density (DD) was about 0.8 km/km², which is a low value for density in a rocky region. The average catchment slope was also low (< 10%), excepting only one very steep catchment (35740000) (slope > 20%). Available Water Capacity (AWC) presented an average of 75 mm and a standard deviation of 11 mm, which is

related to the shallow soil in the study area. Average Runoff Curve Number (CN) was intermediate (77).

Table 3 - Average physiographic characteristics of the selected streamgauge catchments.

| Streamgauge | Cryst (%) | Kc | DD (km/km$^2$) | AWC (mm) | Slope (%) | CN |
|---|---|---|---|---|---|---|
| 34740000 | 0 | 2.17 | 0.62 | 55.5 | 7.2 | 76.9 |
| 35050000 | 44 | 2.01 | 0.61 | 56.6 | 9.2 | 75.3 |
| 35125000 | 93 | 1.81 | 1.00 | 66.0 | 8.0 | 76.7 |
| 35170000 | 77 | 2.18 | 0.89 | 68.9 | 8.2 | 76.6 |
| 35210000 | 96 | 2.76 | 1.01 | 74.6 | 7.2 | 76.8 |
| 35260000 | 93 | 2.53 | 0.93 | 60.5 | 7.6 | 76.8 |
| 35275000 | 87 | 2.25 | 0.92 | 67.4 | 7.0 | 76.8 |
| 35370000 | 96 | 2.19 | 0.83 | 61.5 | 6.7 | 77.1 |
| 35650000 | 92 | 2.55 | 0.74 | 74.7 | 8.5 | 76.0 |
| 35740000 | 99 | 2.28 | 0.53 | 109.4 | 22.3 | 79.2 |
| 35880000 | 87 | 2.39 | 0.76 | 85.2 | 8.5 | 76.1 |
| 35950000 | 81 | 2.11 | 0.71 | 85.6 | 3.7 | 75.7 |
| 36020000 | 92 | 2.37 | 0.73 | 76.6 | 5.3 | 76.6 |
| 36045000 | 73 | 2.99 | 0.71 | 75.4 | 6.1 | 76.6 |
| 36070000 | 86 | 2.75 | 0.74 | 70.1 | 6.4 | 76.6 |
| 36125000 | 73 | 2.25 | 0.70 | 84.8 | 8.0 | 76.4 |
| 36130000 | 66 | 2.83 | 0.55 | 92.8 | 8.7 | 76.6 |
| 36160000 | 81 | 2.86 | 0.72 | 75.2 | 7.0 | 76.6 |
| 36210000 | 40 | 2.07 | 0.66 | 97.4 | 7.8 | 77.3 |
| 36250000 | 41 | 3.21 | 0.61 | 71.6 | 5.2 | 76.3 |
| 36260000 | 48 | 2.28 | 0.69 | 81.2 | 6.5 | 76.5 |
| 36270000 | 56 | 2.19 | 0.79 | 75.1 | 6.7 | 76.5 |
| 36290000 | 67 | 2.43 | 0.80 | 78.8 | 6.9 | 76.6 |
| 36320000 | 78 | 2.79 | 0.77 | 76.9 | 7.1 | 76.7 |
| 36390000 | 79 | 2.90 | 0.84 | 74.6 | 6.7 | 76.7 |
| 36470000 | 97 | 2.46 | 1.01 | 75.0 | 8.8 | 77.3 |
| 36520000 | 98 | 2.18 | 1.09 | 64.9 | 8.0 | 77.2 |
| 36580000 | 96 | 2.71 | 0.99 | 69.2 | 7.2 | 77.0 |

Source: Elaborated by the author.

Then, a multiple linear regression based on the aforementioned standardized catchment characteristics and the standardized (dimensionless) long-term precipitation was fitted to the average standardized specific runoff ($q$) (equation 11), whose coefficients were adopted as weights for the K-N-N regionalization approach. The fitted regression presented a coefficient of determination of 0.78 (Figure 9), which may indicate that both the physiographic characteristics and the precipitation are strongly related to the long-term streamflow in the study area.

$$q = 0.325Cryst - 0.020Kc - 0.096DD - 0.208AWC - 0.176Slope + 0.181CN + 1.003P \quad (11)$$

According to the coefficients, the precipitation was the most important variable for the long-term streamflow prediction, as expected. However, some physiographic characteristics showed to be relevant, as the portion area on the crystalline bedrock (*Cryst*), the Available Water Capacity (*AWC*), the Curve Number (*CN*) and the catchment average slope. On the other hand, the influence of the Gravelius Compactness Coefficient (*Kc*) and the drainage density (*DD*) were much less important on the long-term streamflow, and probably on the monthly streamflow as well.

Figure 9 – Comparison between the observation and the average specific runoff based on the multiple linear regression of the physiographic characteristics and the precipitation. The twenty-eight selected streamgauges were taken into account.

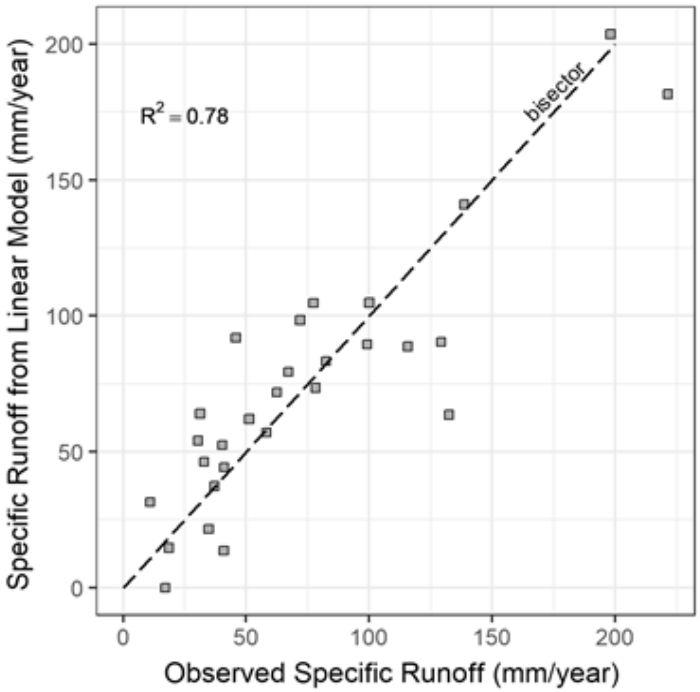


Source: Elaborated by the author.

### *2.5.4 Regionalization application*

For each streamgauge catchment, we determined the five nearest neighbours and the respective set of 1000-value parameter distributions, according to the 1-N-N, 3-N-N and 5-N-N regionalization approach. Then, we calculated streamflow under parametric uncertainty with SMAP, obtaining 1000 series for each analysed catchment. As example, we plotted the streamflow prediction band (5%-95%) for the 36260000 and 34740000 streamgauges (Figure 10). These results were compared to the observed data.

Figure 10 – Streamflow prediction band (5%-95%) for 36260000 and 34740000 streamgauges calculated by SMAP using the regionalized parameters according to 1-N-N, 3-N-N, and 5-N-N.

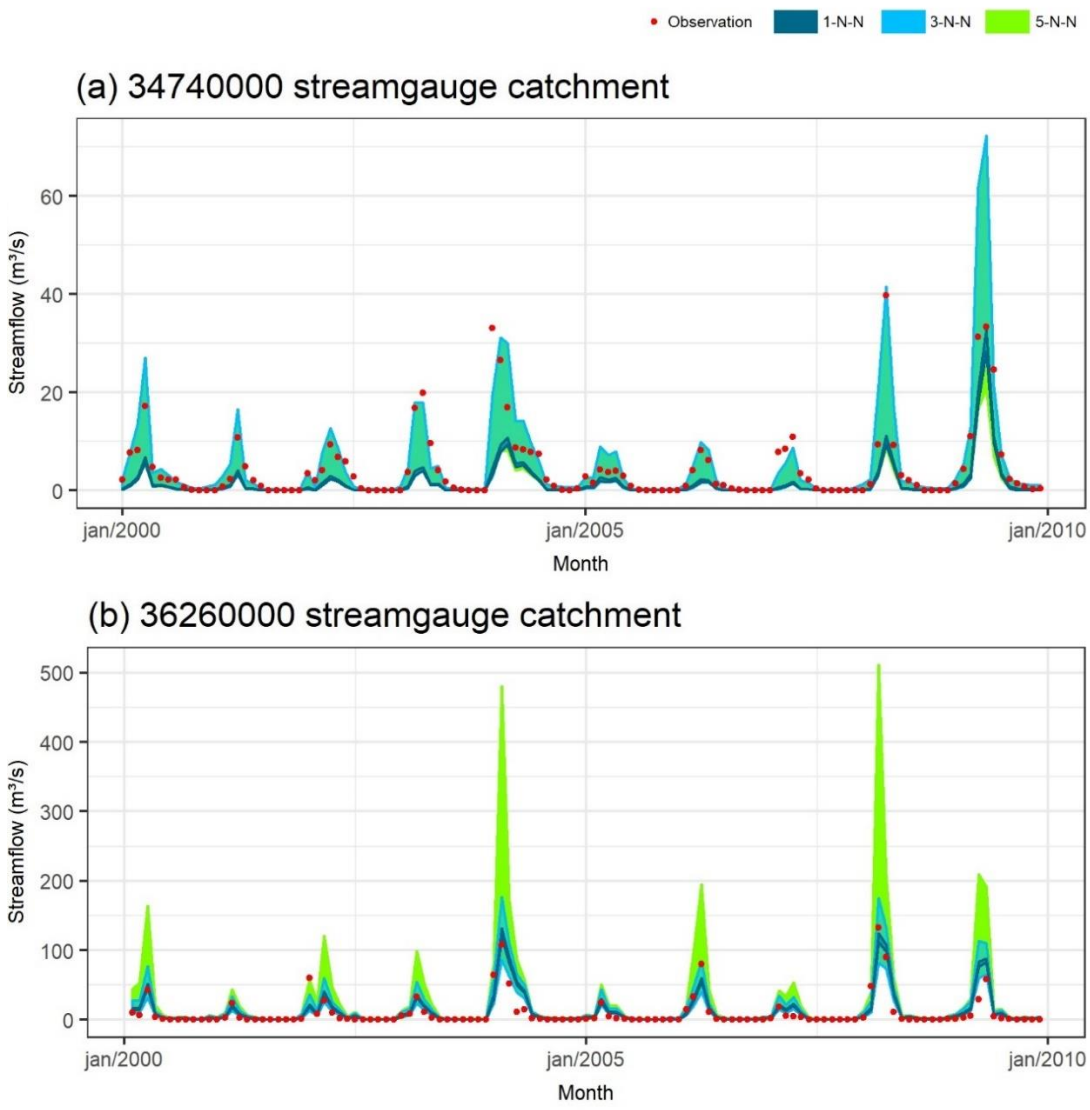


Source: Elaborated by the author.

For the 36260000 streamgauge, which represents the average physiographic conditions in the study area, 1-N-N regionalization captured well most streamflow in the evaluated period, although 3-N-N was necessary to reach some peaks. The prediction band became too large when more neighbours (5-N-N) were used, in exchange of little prediction performance improvement. On the other hand, for the 34740000 streamgauge, whose catchment is the unique completely inside a sedimentary basin, using more neighbours allowed the model to capture many streamflow peaks that were far to be matched by the 1-N-N approach, but it increased considerably the prediction band.

In order to evaluate the performance of the three regionalization approaches for all catchments, we calculated the $NSE$, naming $NSE_{reg\ 1-N-N}$, $NSE_{reg\ 3-N-N}$, and $NSE_{reg\ 5-N-N}$ for the 1-N-N, 3-N-N, and 5-N-N approach, respectively. The $NSE_{val}$ was used as reference for goodness-of-fit of the $NSE_{reg}$ , assuming the validation period for the evaluation of $NSE_{reg}$ as well, since the real-world model assessment was carried out in that period. The Figure 11 shows the overall NSE results, providing its average and its standard deviation for 1-N-N, 3-N-N, and 5-N-N approaches, and for using just the catchment calibrated parameters (validation).

Average $NSE_{reg}$ were 0.55, 0.62 and 0.67 for 1-N-N, 3-N-N, and 5-N-N, respectively. For most streamgauges, average $NSE_{reg}$ was also close to the respective average $NSE_{val}$, and in some cases $NSE_{reg}$ values were even higher than the $NSE_{val}$, which showed that developed regionalization strategy worked well for the study area.

Even if for few streamgauges (e.g. 34740000, and 36580000) 3-N-N and 5-N-N provided on average more accurate prediction than 1-N-N, we found a consistent deterioration of the prediction performance with the increasing number of neighbours for most of streamgauges (e.g. 35740000, 36210000, and 36260000). Moreover, in these cases, the $NSE_{reg\ 3-N-N}$ and $NSE_{reg\ 5-N-N}$ variability became quite higher, leading to large model uncertainty.

Figure 11– Overall NSE results: average and standard deviation from 1-N-N, 3-N-N, and 5-N-N approaches, and from using just the catchment calibrated parameters (validation). Only the validation period was considered in the $NSE$ evaluations.

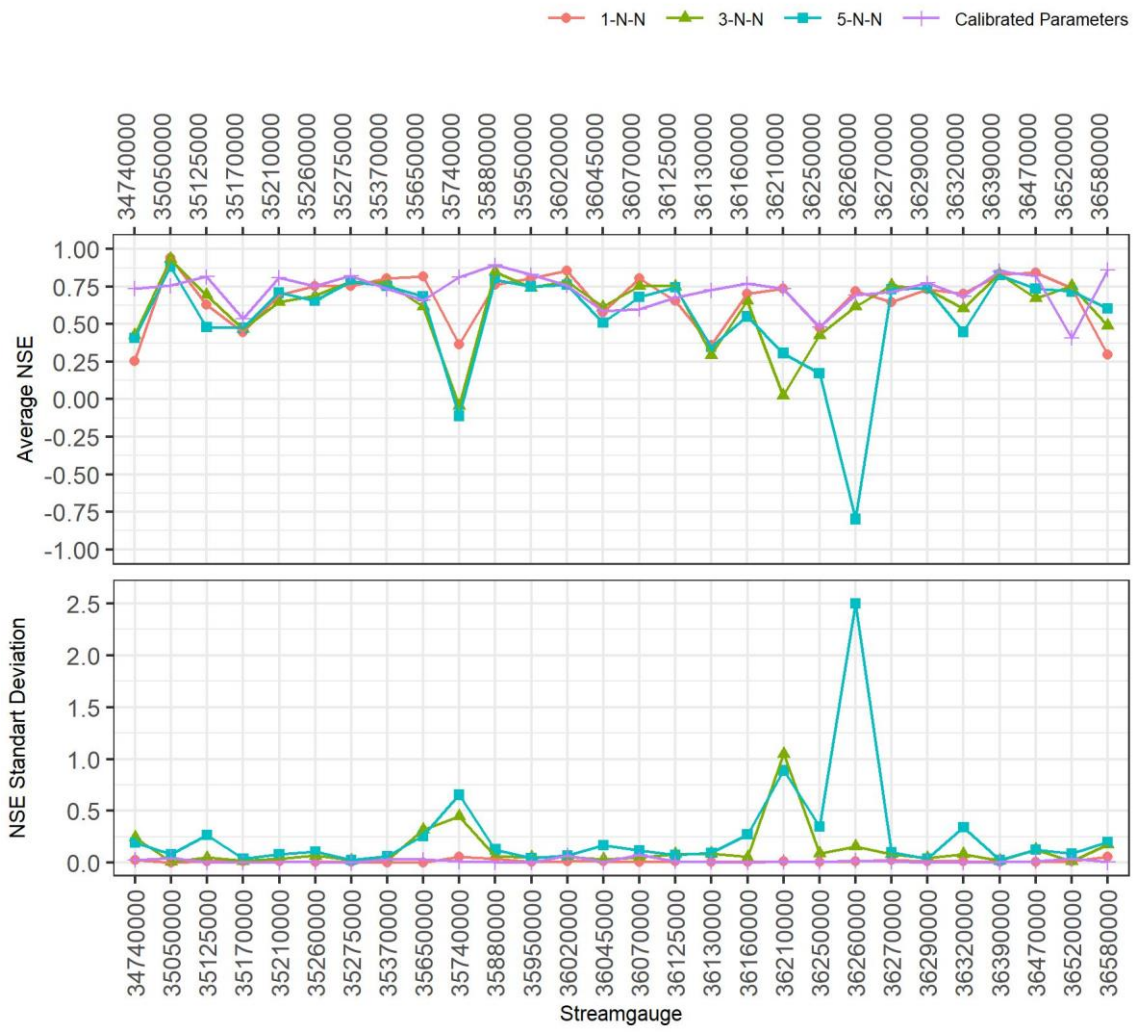


Source: Elaborated by the author.

Table 4 - Number of streamgauges distributed in classes according to the absolute difference between the average values of $NSE_{reg}$ and $NSE_{val}$ (Δ), considering the three regionalization approaches (1-N-N, 3-N-N and 5-N-N).

| **Number of Neighbours** | **Class** | | | | |
|---|---|---|---|---|---|
| | $\Delta \leq 0.05$ | $0.05 < \Delta \leq 0.2$ | $0.2 < \Delta \leq 0.6$ | $\Delta > 0.6$ | Total |
| 1-N-N | 11 | 11 | 6 | 0 | **28** |
| 3-N-N | 9 | 13 | 4 | 2 | **28** |
| 5-N-N | 7 | 10 | 9 | 2 | **28** |

Source: Elaborated by the author.

## 2.6 Conclusion

In this study, we estimated the parameter model uncertainty for twenty-eight streamgauge catchments in the State of Ceará, NE Brazil, and we proposed a regionalization approach, which was based on the K-Nearest-Neighbours classification, to predict streamflow and to assess the uncertainty in ungauged catchments.

The considered physiographic characteristics in the similarity assessment of the catchments provided a satisfactory estimation of the model parameters. The K-Nearest-Neighbours regionalization produced accurate streamflow prediction with an average $NSE$ of 0.67, when only the first neighbour is used. In fact, results showed that the first nearest neighbour frequently was a parameter predictor better than a combination of the three or five nearest neighbours, which can significantly increase the uncertainty of streamflow prediction. The uncertainty band generated by regionalized parameters allowed to capture more observed streamflow data, leading to a better representation of streamflow states than the calibrated parameters for some catchments.

The framework developed in this study allows to assess uncertainty of rainfall-runoff models due to parameter equifinality to ungauged catchments, considering explicitly this uncertainty in the regionalization. This approach also represents a very relevant tool to be applied for the water resources management in the State of Ceará, providing inflow prediction to the main reservoirs and their associated uncertainties. Besides it may be useful for other similar dryland regions in the world.

# 3 SECOND ARTICLE

**Assessment of a hydrosystem water availability: a comparison between parameter and climate change uncertainties, using CMIP6 models.**

**Abstract**:
Climate change is expected to induce extensive socioeconomic consequences. However, only a few studies have assessed the impact of climate change uncertainties on water availability of complex reservoir network systems. In this study, we propagated climate change and model parameter uncertainties in water availability simulation of the Jaguaribe-Metropolitan hydrossystem, in Brazilian northeast. Eight Global Circulation Models (GCMs) from the sixth phase of Coupled Model Intercomparison Project (CMIP6) were used to represent future climate. Differential Evolution Adaptive Metropolis (DREAM) was used to assess parameter uncertainty, propagated to ungauged reservoir drainage areas with a K-Nearest-Neighbor regionalization approach. Half of GCMs indicated a significant increase in water availability for the period between 2021 and 2050, while the other half indicated decrease or no significant change. Parameter uncertainty showed to be negligible in comparison to climate change uncertainty.

Keywords: Climate change, CMIP6, water availability, parameter uncertainty.

## 3.1 Introduction

Remarkable climate-driven alterations in the occurrence of hydrologic variables have been described by the scientific literature in the last decades, e.g. precipitation and streamflow trends; changes in the magnitude and frequency of droughts and floods; and water availability (BURN; HAG ELNUR, 2002; GROISMAN *et al.*, 2004; HAMLET *et al.*, 2007; KHATTAK; BABEL; SHARIF, 2011; PETROW; MERZ, 2009; ROOD *et al.*, 2008). Water resources alterations related to hydroclimatic changes may have extensive environmental and socioeconomic impacts and must be considered for a better long-term planning and management (BUYTAERT *et al.*, 2010; DÖLL *et al.*, 2014; IGLESIAS; GARROTE, 2015; KHATTAK; BABEL; SHARIF, 2011; MIDDELKOOP *et al.*, 2001; MILLY *et al.*, 2008; POFF *et al.*, 2016; ROOD *et al.*, 2008). Despite the growing scientific interest, the modelling and quantification of these changes are still subject to high uncertainty (CLARK *et al.*, 2016; KUNDZEWICZ *et al.*, 2018; MAIER *et al.*, 2016; RAJE; KRISHNAN, 2012). Managers need to assess these uncertainties in their decisions to efficiently increase the reliability and the adaptation of the hydrosystems to climate change impacts (BORGOMEO *et al.*, 2014; HER *et al.*, 2019; MINVILLE; BRISSETTE; LECONTE, 2010).

The uncertainty in future streamflow modelling arise mainly from: i) the long-term simulation of climatological variables (e.g. precipitation, temperature and wind speed) by General Circulation Models (GCMs); ii) the transformation of the future climate variables into future runoff by hydrologic models; and iii) the downscaling of the climatological forcing. The first two are going to be discussed in this research.

The first, climate uncertainty, is related to the choice of the GCMs, the greenhouse emission scenarios and horizons (POFF *et al.*, 2016; VETTER *et al.*, 2017). These scenarios are related to radiative forcing, a variable that quantifies Earth energy flux changes driven by climate change. There are several GCMs developed by different research institutions, each with its own premises, physical formulation and resolutions. The GCMs are brought together as part of the Coupled Model Intercomparison Project (CMIP) (MEEHL *et al.*, 2000) that is in its sixth phase, the CMIP6 (EYRING *et al.*, 2016). The climate uncertainty is traditionally quantified by considering a multi-GCM ensemble with the spread between the members as the amount of uncertainty (KNUTTI *et al.*, 2010; MURPHY *et al.*, 2004; PARKER, 2010). Despite the limitations and the spread of results from different GCMs, they remain the only reliable manner for long-term simulating climate variables (HER *et al.*, 2019; MURPHY *et al.*, 2004; RAJE; KRISHNAN, 2012; WIDÉN-NILSSON; HALLDIN; XU, 2007).

The second source of uncertainty, the hydrologic uncertainty, depends on the choice of the hydrologic model structure and the equifinality of its parameters (BASTOLA; MURPHY; SWEENEY, 2011; HER; CHAUBEY, 2015; POFF *et al.*, 2016). The structure defines how, and which processes are represented. Although complex hydrologic models can reproduce more specific processes, they require more parameters and larger datasets that can increase the uncertainty. Thus, the model structure is often determined based on data availability and the required information. Simpler models with acceptable performance are preferable (HER *et al.*, 2019).

Parameter uncertainty or equifinality consists in the existence of multiple parameter sets that result in hydrologic models with similar performance in calibration. Equifinality results in parameter non-identifiability and it is an inevitable source of hydrological modelling uncertainty (BEVEN, 2006; HER; CHAUBEY, 2015). Equifinality is often quantified using a Bayesian approach, which considers model parameters as random variables, estimating its probability distribution through observed data assimilation. Formal and informal Bayesian-inference-based algorithms have been developed on the last decades (VRUGT *et al.*, 2009). For instance, the Generalized Likelihood Uncertainty Estimation (GLUE), proposed by Beven and Binley (1992), assess parameter uncertainty in an informal approach. Vrugt *et al.* (2008) developed the Differential Evolution Adaptive Metropolis (DREAM), a Markov Chain Monte Carlo (MCMC) scheme that allows formal assessment of parameter uncertainty in model calibration. GLUE and DREAM present similar performance. However, DREAM attempts to disentangle the effect of equifinality from the others predictive uncertainties in modal calibration (VRUGT *et al.*, 2009).

Some studies compared parameter and climate change uncertainties (HER *et al.*, 2019; LUDWIG *et al.*, 2009). According to Ludwig *et al.* (2009), hydrological models generate more uncertainties than GCMs. Her *et al.* (2019), in turn, found out that climate uncertainty has a more relevant effect on rapid hydrological components, while equifinality is dominant for slow components. They also found that GCMs uncertainties are larger in precipitation projections than in temperature.

All these studies focus on hydro climatological variables (e.g. streamflow, precipitation and evapotranspiration) and none have addressed the impact of the uncertainty of future climate modelling on water resources management.

Another practical issue is how to address these uncertainties to ungauged catchments. In this regard, Estacio *et al.* (2020) proposed, in an unpublished work, a methodology to propagate parameter uncertainty from gauged to ungauged catchments. This

methodology, reproduced here, uses a K-Nearest-Neighbor (K-N-N) regionalization approach combined with DREAM to assess parameter uncertainty.

In this study, we assessed the uncertainty in streamflow modelling under climate change, and its impacts in the performance of a reservoir system operation and in water availability. For this, we coupled the traditional methodology for future climate uncertainty assessment (i.e. considering different GMC and scenarios for the climate uncertainty), and the Bayesian MCMC approach to the hydrogical model parameters uncertainty, using the framework and outcomes from Estacio *et al.* (2020). These uncertainties were propagated into a reservoir system operation model, in order to assess its water availability in climate change conditions. We also assessed the hydrosystem water availability in the 20$^{th}$ century climate conditions. The Jaguaribe-Metropolitan hydrossystem in the State of Ceará, Brazil, was considered as case study.

## 3.2 Study area hydro-climatology and hydraulic infrastructure

Jaguaribe basin (75,669 km²) is located in the northeast of Brazil between 4º 30' S and 7º 45' S latitudes and 37º 30' W and 41º 00' W longitudes. Its main river, Jaguaribe, is the biggest in the Brazilian Oriental Atlantic Northeast Hydrographic Region, and the most important water resource in State of Ceará, accounting for 72% of its reservoir storage capacity (SOUZA FILHO, 2018).

Hydro-climatology of the region is marked by high annual and interannual variability, with a six month dry season and frequent pluriannual droughts (SOUZA FILHO, 2018). Annual rainfall ranges from 500 mm to 1200 mm, with 75% of total amount concentrated in 4 months of the year (February–May) (GONDIM *et al.*, 2018). Average temperatures are high (24 – 27 ºC) in the four seasons. High potential evapotranspiration rates (>1500 mm/year) result in a water deficit ranging from 500 to 1200 mm/ year (INSTITUTO BRASILEIRO DE GEOGRAFIA E ESTATÍSTICA (IBGE), 1999).

The shallow soils of the region, situated mainly on crystalline bedrock (80%), result in scarce groundwater resources. For this reason, the construction of surface reservoirs was the main strategy adopted by local government to provide water for multiple uses (SOUZA FILHO, 2018).

The three biggest reservoirs in Ceará, Castanhão (6.70 billion m³), Orós (1.94 billion m³) and Banabuiú (1.60 billion m³), are located in Jaguaribe basin. They represent 55%

of total storage capacity of Ceará reservoirs (18.60 billion m³), and 79% of the basin (13.00 billion m³) (ANA, 2017).

Channels connect Jaguaribe basin to smaller reservoirs in Metropolitan Area of Fortaleza (MAF). These reservoirs supply drinking water for 4 million people in MAF, besides attending water demands of local industries. Jaguaribe-Metropolitan reservoirs and channels form the Jaguaribe-Metropolitan hydrossystem.

The study area (Figure 12) occupies 65,310 km², including Castanhão, Orós and Banabuiú catchments, and the catchments of other five reservoirs in MAF (Aracoiaba, Gavião, Pacajus, Pacoti-Riachão and Sítios-Novos).

Because Castanhão and Pacajus are downstream from Orós and Aracoiaba, respectively (see Figure 12), for the first two we considered the incremental drainage areas (and not the total catchment) in rainfall-runoff modelling.

Figure 12 – Catchment area of the reservoirs in the study area.

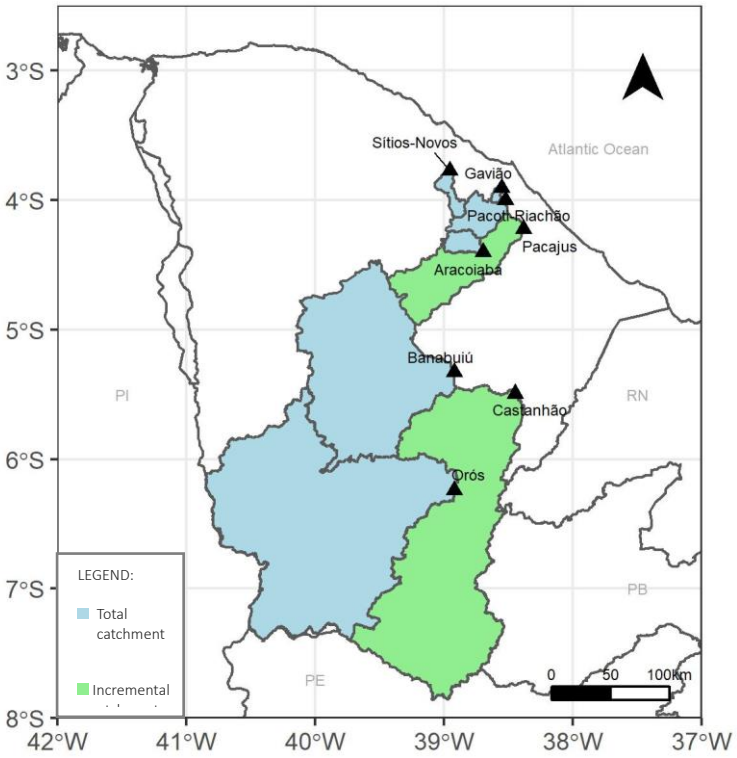


Source: Elaborated by the author.

## 3.3 General framework

The proposed framework (Figure 13) allows to assess Jaguaribe-Metropolitan hydrossystem water availability in both present (20th century) and future climate conditions, incorporating parameter and climate change uncertainties. For this, we simulated streamflow in the reservoir catchments with observed climate data and projections from eight GCMs from CMIP6. The rainfall-runoff model was the monthly Soil Moisture Accounting Procedure (SMAP), a conceptual lumped model, which has been frequently applied for water resources assessment in Brazil.

Parameters of SMAP were obtained using a K-N-N regionalization approach, proposed by Estacio *et al.* (2020), which assimilates parameter uncertainty in model calibration and allows to propagate it from gauged catchments to ungauged ones. Through this approach, we obtained a set of parameters that represent equifinality. Simulation of reservoir operation was used to estimate the water availability of the eight targeted reservoirs.

Figure 13 – Proposed framework for water availability assessment under parameter and climate change uncertainties.

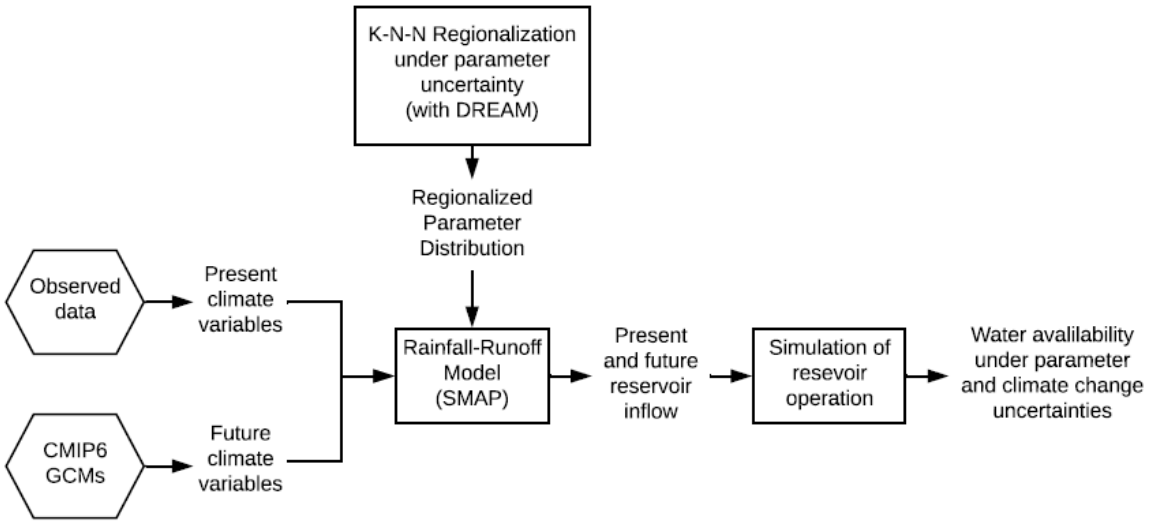


Source: Elaborated by the author.

### 3.4 Precipitation and evapotranspiration data for the present climate (20th century)

Precipitation representing present climate was obtained from the records from 815 rain gauges, provided by the Brazilian National Water Agency (ANA). An inverse distance weighting approach (PLOUFFE; ROBERTSON; CHANDRAPALA, 2015) was used to interpolate local precipitation from the gauges to the targeted reservoir catchment areas. Monthly precipitation series were calculated from 1910 to 2017. This data was assumed to represent 20th century precipitation regime.

Potential evapotranspiration was calculated with the Hargreaves-Samani equation, which estimates it from temperature and latitude. Temperature data was obtained from the meteorological data processed by Xavier, King and Scanlon (2016). Monthly evapotranspiration was interpolated from stations into the catchments with a weighting average using the Thiessen polygons.

### 3.5 CMIP6 climate change models and scenarios

In its sixth phase, the Coupled Model Intercomparison Project (i.e. CMIP6) proposed a new integrated structure that attempts to respond the major required improvements identified in the previous editions (EYRING *et al.*, 2016). With the first model simulations in 2016 (EYRING *et al.*, 2016), CMIP6 has released, since then, historical and projection outputs for a couple of GCMs.

In this study we considered eight recent models (Table 5) from CMIP6 dataset to represent the climate change uncertainty that may impact water availability.

Table 5 - Global Circulation Models from CMIP6 considered in the study and its respective sources.

| Model | Source |
|---|---|
| BCC-CSM2-MR | (WU *et al.*, 2018) |
| CanESM5 | (SWART *et al.*, 2019) |
| FGOALS-g3 | (LI, 2019) |
| IPSL-CM6A-LR | (BOUCHER *et al.*, 2018) |
| MIROC6 | (TATEBE; WATANABE, 2018) |
| MPI-ESM1-2-HR | (VON STORCH *et al.*, 2017) |
| MRI-ESM2-0 | (YUKIMOTO *et al.*, 2019) |
| NESM3 | (CAO, 2019) |

Source: Elaborated by the author.

Scenario Model Intercomparison Project (ScenarioMIP) defines standard possible climate forcing pathways within CMIP6 and uses the same emission scenarios for the ensemble of GCMs. Each one of these projections were designed in collaboration with the scientific community, considering different pathways for the global development (O'NEILL *et al.*, 2014). We considered two Shared Socioeconomic Pathways (SSP) designed by ScenarioMIP: SSP2-4.5 and SSP5-8.5.

In SSP2-4.5, historical tendencies of global development are maintained, with an intermediate radiative forcing (4.5 W/m²). SSP5-8.5, in turn, considers intense socioeconomical development based on the exploitation of fossil fuel, producing a higher radiative forcing (i.e. 8.5 W/m²) (O'NEILL *et al.*, 2014).

Monthly precipitation and temperature for the next thirty years (2021-2050) were calculated from GCMs forecasts for both scenarios. All consideration of future condition in this study considers this thirty-year period. Thiessen polygons were used to interpolate the climate variable projections from GMSs grids to catchments area.

A bias-correction procedure was performed to reduce the interpolation errors and inaccuracies inherent to GCMs. For this, we compared historical outputs of the GCMs to the observed data, assuming the models would reproduce the same pattern in prediction errors. Thus, the same bias-correction used in historical projections was used for future climatic projections. Historical and observed precipitation data comprise the period from 1911 to 2014, and temperature, from 1980 to 2013. We corrected precipitation using a gamma-gamma transformation (SHARMA; BABEL, 2018), which was applied to each month, correcting also the seasonality. For temperature, we used the monthly mean correction, which presented accurate results (SALVI; KANNAN; GHOSH, 2011). Potential evapotranspiration in future conditions (2021-2050) was calculated from corrected temperature using the Hargreaves-Samani equation.

### *3.5.1 Rainfall-runoff model, regionalization and parameter uncertainty*

We used Soil Moisture Accounting Procedure (SMAP), a conceptual lumped rainfall-runoff model (FERNANDES *et al.*, 2017; LOPES; BRAGA; CONEJO, 1981; SILVEIRA; SOUZA FILHO; VASCONCELOS JÚNIOR, 2017), to obtain the reservoir inflows produced in the catchments in the present (20$^{th}$ century) and future (2021-2050) conditions.

Since we wanted to assess the long-term water availability, we chose the monthly version of SMAP, which represents the flows in the watershed through soil and underground reservoirs. The monthly version of SMAP has four parameters, named $SAT$, $PES$, $CREC$ and $K$, controlling internal water fluxes and outputs.

SMAP could not be calibrated for the catchments, because there are no records of the reservoirs inflow. Instead, we used a regionalization method to estimate SMAP parameters for the catchments. The parameter regionalization was based on the K-Nearest-Neighbor algorithm, proposed in an unpublished study by Estacio *et al.* (2020). The method estimates the parameters of the rainfall-runoff model in ungauged catchments based on the similarity with the gauged catchments in the region. Estacio *et al.* (2020) selected twenty-eight streamgages in the State of Ceará as donor catchments and used monthly SMAP. We considered only one donor catchment in the regionalization, which gives best estimation of parameters (ESTACIO *et al.*, 2020).

Estacio *et al.* (2020) considered parameter uncertainty and propagated it to the ungauged catchments through the regionalization. The proposed framework calibrated the gauged catchments using the Differential Evolution Adaptive Metropolis (DREAM), a Markov chain Monte Carlo (MCMC) sampler that can be used to simultaneously calibrate models and determine parameter uncertainty based on Bayesian inference (VRUGT *et al.*, 2008).

Using this regionalization approach, we obtained for each reservoir catchment a set of 1000 values of the four parameters of SMAP, representing the parameter uncertainty. Then, we calculated the reservoir inflows, obtaining 1000 series for each catchment, considering 20$^{th}$ century climate conditions and GCM projections for future climate (2021-2050). In order to assess climate uncertainty without parameter uncertainty effect, we also considered the inflow series generated using median parameters.

### *3.5.2 Hydrosystem simulation and water availability assessment*

The targeted reservoir networks, including monitored reservoirs upstream the targeted one (Figure 14), were simulated, in order to incorporate the hydrosystem efficiency in the water availability assessment. Only Gavião and Pacoti-Riachão reservoirs do not present other upstream monitored reservoirs. The channels of Jaguaribe-Metropolitan hydrosystem were not modeled, since their only function is transfer water between reservoirs, while this study focus on the hydrosystem global water availability. Total inflow produced in the targeted

reservoir catchments was calculated with SMAP and distributed to the incremental draining areas of each reservoir.

Reservoirs upstream the targeted one were operated in simulations with the official draw-off discharges that can be granted for them, according to the Water Resources Office of State of Ceará (SRH-CE). A sensitivity analysis has shown for the reservoir networks of the region the draw-off rate of upstream reservoirs does not strongly affect the yield of the downstream reservoir (ESTACIO; SOUZA FILHO; PORTO, 2018). In fact, since streamflow regime in the study area concentrate flow in a short period of the year, most inflow of smaller reservoirs spills. On the other hand, the evaporation in these reservoirs represent a relevant portion of the water balance in the hydrosystem. Consequently, simulating the whole network is necessary to fairly represent this balance (ESTACIO; SOUZA FILHO; PORTO, 2018).

Then, we calculated the individual inflow of the reservoirs in simulations by adding the drainage volume of the incremental watershed to the spills of the immediately upstream reservoirs.

Figure 14 – Targeted reservoir networks of Jaguaribe Metropolitan hydrosystem.

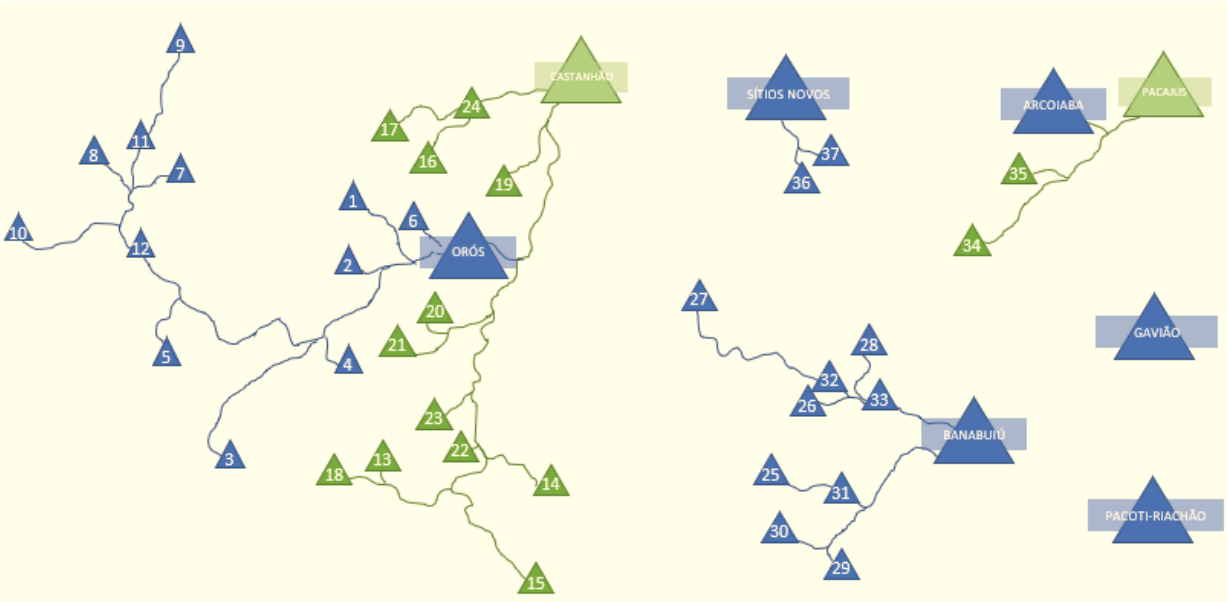


| MINOR RESERVOIRS | | | | |
|---|---|---|---|---|
| 1- Quincoé | 10- Parambu | 17 – Jenipapeiro | 24- Riacho do Sangue | 31- Patu |
| 2- Trussu | 11-Varzea do Boi | 18- Thomás Osterne | 25- Trapia II | 32-Fogareiro |
| 3- Canoas | 12-Arneiroz II | 19- Joaqui Távora | 26- São José I | 33- Quixeramobim |
| 4- Muquém | 13-Manual Balbino | 20- Tatajuba | 27- Monsenhor Tabosa | 34- Pompeu Sobrinho |
| 5- Benguê | 14-Prazeres | 21-Ubaldinho | 28- Pirabibu | 35- Catro |
| 6- Faé | 15- Quixabinha | 22- Cachoeira | 29- São José II | 36- Itapebussu |
| 7- Favelas | 16 – Tigre | 23- Rosário | 30- Serafim Dias | 37- Amanary |
| 8- Triçi | 10- Parambu | 17 – Jenipapeiro | 24- Riacho do Sangue | 31- Patu |
| 9- Forquilha II | 11-Varzea do Boi | 18- Thomás Osterne | 25- Trapia II | 32-Fogareiro |

Source: Elaborated by the author.

The water balance in the reservoirs was calculated according to the mass conservation equation (12). The reservoir storage variation $\left(\frac{\mathrm{dV}}{\mathrm{dt}}\right)$ was calculated as the difference between inflow (A) and outflows. The main outflows considered in the simulations consist of the discharge drawn from the reservoir (D), spills (Sp), and evaporated discharge, which was calculated as the product of the evaporation rate (E) and the surface area of the reservoir S(V).

$$\frac{dV}{dt} = A - D - Sp - E \times S(V) \tag{12}$$

The elevation-area-capacity curves of the reservoirs, provided by Ceará Water Resources Management Company (COGERH), allow to consider surface area variations with the storage. Piché evaporimeter data from the nearest meteorological station of Brazilian Institute of Meteorology (IMET) was used to calculate evaporation rates in the reservoirs. In the future climate conditions, the increase in evaporation was considered at the same rate as the increase in evapotranspiration, calculated from bias-corrected temperature from the GCMs.

Then, we calculated the long-term discharge that can be drawn with 90% of reliability (Q90). This value is a reference for reservoirs maximum discharge that can be granted according to local law (CAMPOS; SOUZA FILHO; LIMA, 2014). We adopted Q90 as the measure of water availability to be assessed in this work.

The parameter uncertainty was taken account into Q90 evaluation by considering the 1000 streamflow series that resulted from parameter uncertainty. Thus, we found out 1000 values of Q90 for each catchment in 20$^{th}$ century and for each GCM in both scenarios. Climate uncertainty was assessed by the ensemble of models and scenarios. We also calculated Q90 using the streamflow series generated by the median parameter. In this way, we isolated climate uncertainty from parameter uncertainty.

Since two targeted reservoirs (i.e. Castanhão and Pacajus) presented other targeted reservoirs upstream, a particular framework was developed to simulate these reservoir networks, considering the upstream targeted reservoir network (i.e. Orós and Aracoiaba networks) and the reservoirs in the incremental area of Castanhão and Pacajus (green reservoirs in Figure 14). From parameter uncertainty, we generated 1000 streamflow series for both incremental and upstream catchment. Thus, we randomly selected 1000 out of $10^6$ (1000 times 1000) combinations of streamflow series for both catchments, keeping the original statistics of likely streamflow series. Then, we calculated Q90 as previously.

## 3.6 Results and discussion

### *3.6.1 Present (20th century) and future (2021-2050) water availability*

Figure 15 shows the average Q90 and the respective coefficient of variation (CV) in 20th century and for each GCM in both scenarios. CV values varied from 0.02 to 0.17, indicating that parameter uncertainty propagated to Q90 results in a Q90 standard deviation with 2%-17% of the average. Moreover, present and future CV, considering each GCM separately, seem to be similar, with any general tendency of increase or decrease, due to climate change, which means that parameter uncertainty was conserved in the simulated scenarios. This result came from the fact that we used the same set of parameters for all simulations, ignoring any land use and cover changes.

On the other hand, for most reservoirs, such Aracoiaba, Castanhão, Orós and Sítios Novos, CV tends to increase as the Q90 average decreases, meaning that smaller Q90 present relatively a larger (but not necessarily less accurate) prediction band.

Figure 15 – Average and coefficient of variation of Q90 for the main reservoirs of JMS in present (20th century) climate conditions and future (2021-2050) climate conditions according to eight GCMs in two scenarios.

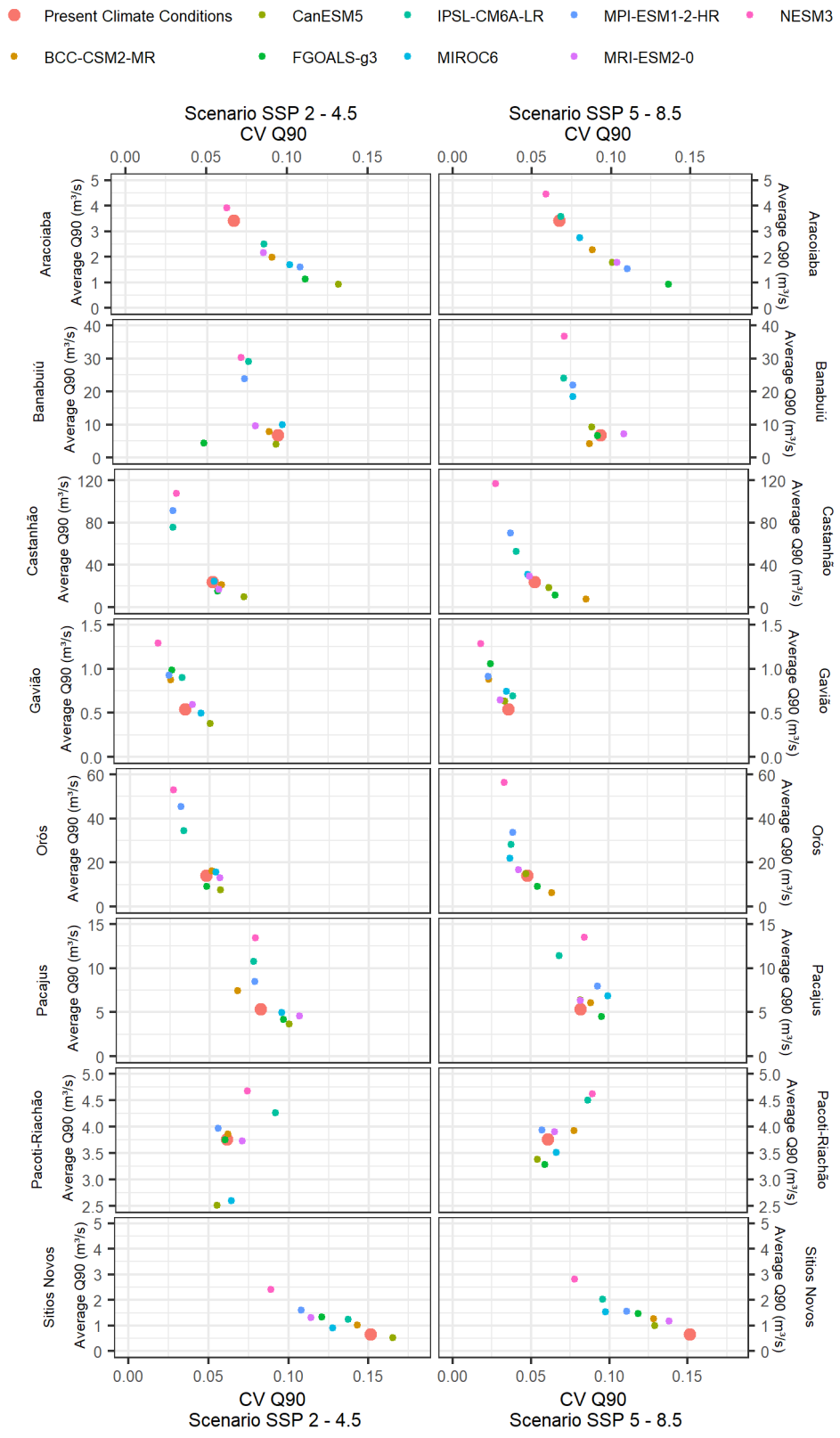


Source: Elaborated by the author.

The relative anomalies in the average Q90 (Figure 16) varied significantly with GCMs and scenarios. According to seven of the eight GCMs, Aracoiaba water availability is going to decrease (73% maximum), while Sítios Novos Q90 are going to increase (320% maximum). For the other reservoirs, including Castanhão, Orós e Banabuiú, nearly half of GCMs indicate an increase of water availability, while the rest projects a decrease or maintenance of Q90 value.

Figure 16 – Average Q90 relative anomalies for the main reservoirs of JMS according to eight GCMs in two scenarios.


Source: Elaborated by the author.

MIROC6 and NESM3 increased the average Q90 from scenario SSP 2 – 4.5 to SSP 5 – 8.5, while BCC-CSM2-MR, IPSL-CM6A-LR, and MPI-ESM1-2-HR decreased. The other models approximately kept the average Q90. Surprisingly, the biggest anomalies are observed for the larger reservoirs.

The positive anomalies are more significant than the negative ones, which could indicate an increase of water availability for the reservoirs of JMS. These results contrasts with the outcomes found out by Gondim *et al.*(2018), who assessed water avaliability in Jaguaribe basin, using CMIP5 models for the period 2025-2055. In the later, most GCMs indicate decrease in water availability.

### *3.6.2 Parameter and Climate Change uncertainties*

Since climate change uncertainty emerge from the ensemble of GCM projectios, we also evaluate together the eight GCM responses propagated to Q90. Thus, we assessed the distribution of these responses in two case studies, considering: (1) the whole set of parameters, which allow to combine parameter and climate change uncertainty; and (2) the median parameters, in order to isolate climate change uncertainty. Q90 distributions for both case studies were analyzed using their boxplots (Figure 17)

For all reservoirs and in both scenarios, Q90 considering only climate change uncertainties presented a similar median as Q90 for combined uncertainty. Moreover, Q90 for combined uncertainty is only slightly more spread than the former. That difference is probably due the added parameter uncertainty, which adds dispersion to Q90 distribution. However, that result is not conclusive, since Q90 sets in both case studies are not equally sized.

Figure 17 – Analysis of climate change and combined (climate change and parameter) uncertainties: Q90 boxplots for the main reservoirs of JMS in two scenarios.

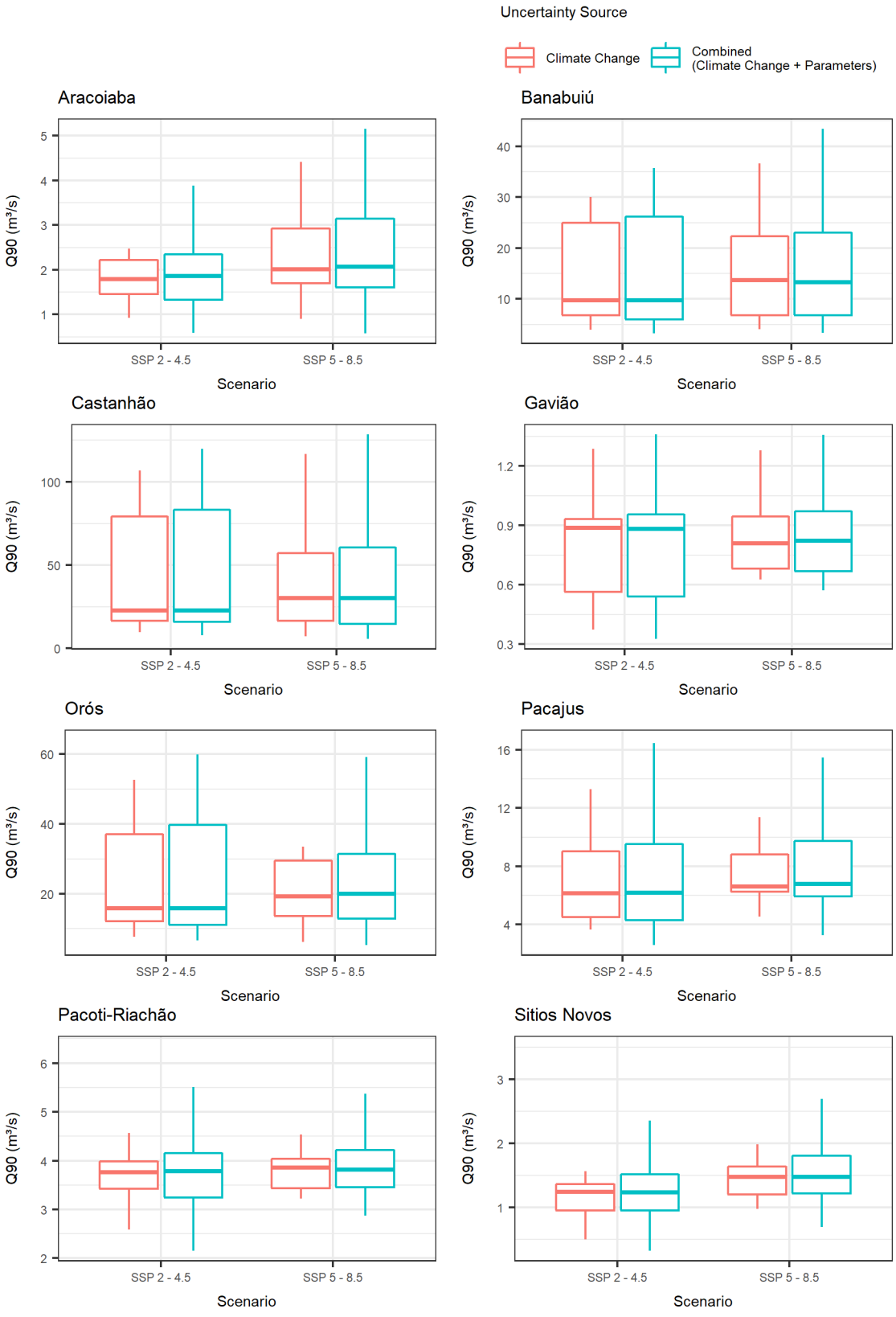


Source: Elaborated by the author.

In order to compare Q90 spread, as a measure of uncertainty in both case studies (climate change and combined uncertainties), we performed a statistic test. Classical Levene's test allow to compare two data set variances, with null hypothesis of homoscedasticity (i.e. no difference between variances) (LEVENE, 1960). We performed this test assuming a significance level of 0.05, and found out the following p-values:

Table 6- p-values for Levene's test to compare Q90 variance from climate change uncertainty analysis and combined uncertainty analysis.

| **p-values** | **Scenario** | |
|---|---|---|
| **Reservoir** | SSP 2 - 4.5 | SSP 5 - 8.5 |
| Aracoiaba | 0.91 | 0.95 |
| Banabuiú | 0.96 | 0.99 |
| Castanhão | 0.95 | 0.99 |
| Gavião | 1 | 1 |
| Orós | 0.96 | 0.98 |
| Pacajus | 0.9 | 0.87 |
| Pacoti-Riachão | 0.75 | 0.52 |
| Sítios-Novos | 0.76 | 0.83 |

Source: Elaborated by the author.

There is no statistical evidence to reject the null hypothesis that Q90 variance from climate uncertainty is identical to combined uncertainty one. Thus, under those circumstances, parameter calibration had a minor effect in combined uncertainty, compared to climate change uncertainty.

## 3.7 Conclusions

In this study we propagated climate change and model parameter uncertainties in water availability assessment for a complex hydrosystem. Half of the selected models indicated a significant increase in water availability of the Jaguaribe Metropolitan hydrosystem for the period between 2021 and 2050. The other half indicated a less significant decrease or maintenance of water availability.

The expected increase in water availability of the Jaguaribe Metropolitan hydrosystem contradicts the projections from the GCMs of CMIP5. Including the new GCMs from CMIP6, since they are made available, is recommended. In addition, water availability assessment must include the evaluation of water demand tendencies in addition to the climate change effects.

Adding parameter equifinality to climate change uncertainty showed no statistical evidence of increase of uncertainty in simulated water availability. Thus, climate change projections represent more relevant uncertainties to future water availability in Jaguaribe-Metropolitan, than parameter equifinality. Further research is recommended to compare GCMs projection uncertainties to those produced by climatological forcing downscaling techniques.

CMIP6 has brought together improved GCMs in an integrated system that helps scientists to assess climate change effects under different scenarios. However, uncertainties in the future climate and its effects on society will persist until GCMs fairly represent the complex atmospheric dynamics in global scale.

# 4 CONCLUSION

This study achieved a parameter regionalization approach based on the K-Nearest-Neighbors classification method that is capable to propagate model parameter uncertainty and to predict streamflow to ungauged reservoir catchments in Ceará. Using the regionalized parameters, the water availability in Jaguaribe Metropolitan hydrosystem was assessed in present and future climate conditions under climate change conditions, considering eight CMIP6 GCMs projections.

The K-Nearest-Neighbors regionalization produced accurate streamflow series projections with an average NSE of 0.67 when one donor catchment is used. Results also showed that using one donor catchment frequently resulted in a better performance than using a combination of three or five donor catchments to predict the model parameters.

CMIP6 GCMs projections indicated an average tendency of increase for Jaguaribe Metropolitan hydrosystem water availability. However, including new GCMs projections, since they are made available, is recommended. In addition, water demand scenarios evaluation should be included to a complete water availability assessment.

Climate change projections showed to be a more relevant source of uncertainty in future water availability assessment than parameter non-identifiability, highlighting the need of a continuous improvement of atmospheric dynamic representation by GCMs.

The framework developed in this dissertation is expected to collaborate with uncertainty assessment in Ceará as a tool for water resources planning and management. However, uncertainties in hydrological modelling and its effects on society will persist until a general framework for natural, antrophic, and informational uncertainty quantification is developed.

## REFERENCES

AGÊNCIA NACIONAL DE ÁGUA (ANA). **RESERVATÓRIOS DO SEMIÁRIDO BRASILEIRO Hidrologia, Balanço Hídrico e Operação - Anexo C (Jaguaribe)**. Brasília: [s.n], 2017. Disponível em: https://www.ana.gov.br/noticias/estudo-reservatorios/anexo-c-jaguaribe.pdf.

ALEXANDRE, A. M. B. **Regionalização de vazões máximas, médias e parâmetros de modelos hidrológicos no Estado do Ceará**. 2005. Dissertação (Mestrado em Engenharia Civil) - Centro de Tecnologia, Programa de Pós-Graduação em Engenharia Civil: Recursos Hídricos. Universidade Federal do Ceará, Fortaleza, 2005.

ASFAW, A.; SHUCKSMITH, J.; MACDONALD, K. Parameter Uncertainties in a Conceptual Rainfall-runoff Model and Implications on Surface Water Management and Planning Decisions. **Procedia Engineering**, *[S. l.]*, v. 154, p. 299–307, 2016. DOI: 10.1016/j.proeng.2016.07.479. Disponível em: http://dx.doi.org/10.1016/j.proeng.2016.07.479.

BARROS, F. V. F. **Uso de Algoritmos Evolucionários na Calibração de Modelos Hidrológicos e na Operação de Sistemas de Reservatórios**. 2007. Dissertação (Mestrado em Engenharia Civil) - Centro de Tecnologia, Programa de Pós-Graduação em Engenharia Civil: Recursos Hídricos. Universidade Federal do Ceará, Fortaleza, 2007

BARROS, F. V. F.; MARTINS, E. S. P. R.; NASCIMENTO, L. S. V.; REIS, D. S. Use of Multiobjective Evolutionary Algorithms in Water Resources Engineering. *In*: NEDJAH, N.; DOS SANTOS COELHO, L.; DE MACEDO MOURELLE, L. (org.). **Multi-Objective Swarm Intelligent Systems**. Berlin: Springer, 2010.

BASTOLA, S.; MURPHY, C.; SWEENEY, J. The role of hydrological modelling uncertainties in climate change impact assessments of Irish river catchments. **Advances in Water Resources**, *[S. l.]*, v. 34, n. 5, p. 562–576, 2011. DOI: 10.1016/j.advwatres.2011.01.008. Disponível em: http://dx.doi.org/10.1016/j.advwatres.2011.01.008.

BENNETT, J. C.; WANG, J. Q.; LI, M.; ROBERTSON, D. E.; SCHEPEN, A. Reliable long-range ensemble streamflow forecasts: Combining calibrated climate forecasts with a conceptual runoff model and a staged error model. **Water Resources Research**, *[S. l.]*, v. 52, 2016. DOI: https://doi.org/10.1002/2016WR019193.

BEVEN, K. A manifesto for the equifinality thesis. **Journal of Hydrology**, *[S. l.]*, v. 320, n. 1–2, p. 18–36, 2006. DOI: 10.1016/j.jhydrol.2005.07.007.

BEVEN, K.; BINLEY, A. The future of distributed models: model calibration and uncertainty prediction. **Hydrological Process**, *[S. l.]*, v. 6, n. 3, p. 279–298, 1992.

BLITZSTEIN, J. K.; HWANG, J. **Introduction to Probability**. 2nd. ed. [s.l.] : Chapman & Hall/CRC Texts in Statistical Science, 2019.

BORGOMEO, E.; HALL, J. W.; WATTS, G.; COLQUHOUN, K.; LAMBER, C. Risk-based water resources planning: Incorporating probabilistic nonstationary climate uncertainties.

**Journal of the American Water Resources Association**, *[S. l.]*, v. 5, n. 3, p. 2–2, 2014. DOI: 10.1111/j.1752-1688.1969.tb04897.x.

BOUCHER, O.; DENVIL, S.; CAUBEL, A.; FOUJOLS, M. A. **IPSL IPSL-CM6A-LR model output prepared for CMIP6 CMIP 1pctCO2**Earth System Grid Federation, , 2018. DOI: https://doi.org/10.22033/ESGF/CMIP6.5049.

BURN, D. H.; HAG ELNUR, M. A. Detection of hydrologic trends and variability. **Journal of Hydrology**, *[S. l.]*, v. 255, n. 1–4, p. 107–122, 2002. DOI: 10.1016/S0022-1694(01)00514-5.

BUYTAERT, W.; VUILLE, M.; DEWULF, A.; URRUTIA, R.; KARMALKAR, A.; CÉLLERI, R. Uncertainties in climate change projections and regional downscaling in the tropical Andes: Implications for water resources management. **Hydrology and Earth System Sciences**, *[S. l.]*, v. 14, n. 7, p. 1247–1258, 2010. DOI: 10.5194/hess-14-1247-2010.

CAMPOS, J. N. B.; LIMA NETO, I. E.; STUDART, T. M. C.; NASCIMENTO, L. S. V. Trade-off between reservoir yield and evaporation losses as a function of lake morphology in semi-arid Brazil. **Anais da Academia Brasileira de Ciencias**, *[S. l.]*, v. 88, n. 2, p. 1113–1125, 2016. DOI: 10.1590/0001-3765201620150124.

CAMPOS, J. N. B.; SOUZA FILHO, F. A.; LIMA, H. V. C. Risks and uncertainties in reservoir yield in highly variable intermittent rivers: case of the Castanhão Reservoir in semi-arid Brazil. **Hydrological Sciences Journal**, *[S. l.]*, v. 59, n. 6, p. 1184–1195, 2014. DOI: 10.1080/02626667.2013.836277.

CAO, J. **NUIST NESMv3 model output prepared for CMIP6 ScenarioMIP ssp126**Earth System Grid Federation, , 2019. DOI: https://doi.org/10.22033/ESGF/CMIP6.8780.

CLARK, M. P. et al. Characterizing Uncertainty of the Hydrologic Impacts of Climate Change. **Current Climate Change Reports**, *[S. l.]*, v. 2, n. 2, p. 55–64, 2016. DOI: 10.1007/s40641-016-0034-x. Disponível em: http://dx.doi.org/10.1007/s40641-016-0034-x.

COELLO, C. A.; LECHUGA, M. S. MOPSO: A proposal for multiple objective particle swarm optimization. In: CONGRESS ON EVOLUTIONARY COMPUTATION, 2., 2002, Honolulu. **Proceedings**... Honolulu: IEEE 2002, p. 1051–1056. DOI: 10.1109/CEC.2002.1004388.

COMPANHIA DE GESTÃO DOS RECURSOS HÍDRICOS (COGERH). **Estudos de regionalização de parâmetros de modelo hidrológico chuva-vazão, para as bacias totais e incrementais dos reservatórios monitorados pela COGERH**. Fortaleza: [s.n], 2013.

COSTA, A. C.; BRONSTERT, A.; DE ARAÚJO, J. C. A channel transmission losses model for different dryland rivers. **Hydrology and Earth System Sciences**, *[S. l.]*, v. 16, n. 4, p. 1111–1135, 2012. DOI: 10.5194/hess-16-1111-2012.

COSTA, A. C.; FOERSTER, S.; DE ARAÚJO, J. C.; BRONSTERT, A. Analysis of channel transmission losses in a dryland river reach in north-eastern Brazil using streamflow series, groundwater level series and multi-temporal satellite data. **Hydrological Processes**, *[S. l.]*, v. 27, n. 7, p. 1046–1060, 2013. DOI: 10.1002/hyp.9243.

CUNNINGHAM, P.; DELANY, S. J. **K -Nearest Neighbour ClassifiersMultiple Classifier Systems**. 2007.[s.l: s.n.]. DOI: 10.1016/S0031-3203(00)00099-6.

DÖLL, P. et al. Integrating risks of climate change into water management. **Hydrological Sciences Journal**, *[S. l.]*, v. 60, n. 1, p. 4–13, 2014. DOI: 10.1080/02626667.2014.967250. Disponível em: http://dx.doi.org/10.1080/02626667.2014.967250.

DUAN, Q.; SOROOSHIAN, S.; GUPTA, V. Effective and Efficient Global Optimization. **Water Resources Research**, *[S. l.]*, v. 28, n. 4, p. 1015–1031, 1992.

ENGELAND, K.; STEINSLAND, I.; JOHANSEN, S. S.; PETERSEN-ØVERLEIR, A.; KOLBERG, S. Effects of uncertainties in hydrological modelling. A case study of a mountainous catchment in Southern Norway. **Journal of Hydrology**, *[S. l.]*, v. 536, p. 147–160, 2016. DOI: 10.1016/j.jhydrol.2016.02.036.

ESTACIO, A. B. S.; SOUZA FILHO, F. A. de.; COSTA, A. C.; ROCHA, R. V. **A K-Nearest Neighbor regionalization approach to propagate the parameter uncertainty of a conceptual rainfall-runoff model to ungauged catchments.** *[S. l.]*, 2020.

ESTÁCIO, A. B. S.; SOUZA FILHO, F. A.; PORTO, V. C. **Análise da sustentabilidade hídrica de mananciais do projeto malha d'água.** 2018 Trabalho de conclusão de curso (Graduação em Engenharia Civil) - Centro de Tecnologia, Curso de Engenharia Civil Universidade Federal do Ceará, Fortaleza, 2018.

EYRING, V.; BONY, S.; MEEHL, G. A.; SENIOR, C. A.; STEVENS, B.; STOUFFER, R. J.; TAYLOR, K. E. Overview of the Coupled Model Intercomparison Project Phase 6 (CMIP6) experimental design and organization. **Geoscientific Model Development**, *[S. l.]*, v. 9, n. 5, p. 1937–1958, 2016. DOI: 10.5194/gmd-9-1937-2016.

FERNANDES, R. de O.; SILVEIRA, C. da S.; STUDART, T. M. de C.; SOUZA FILHO, F. A. Reservoir yield intercomparison of large dams in Jaguaribe Basin-CE in climate change scenarios. **Rbrh**, *[S. l.]*, v. 22, n. 0, 2017. DOI: 10.1590/2318-0331.011716033.

FOGEL, D. B. The Advantages of Evolutionary Computation. **Applications of Soft Computing**, *[S. l.]*, v. 3165, n. 1995, p. 14–22, 1997. DOI: 10.1117/12.279591.

FRISCHKORN, H.; SANTIAGO, M. F.; DE ARAUJO, J. C. Water Resources of Ceará and Piauí. *In*: T. GAISER, M. KROL, H. FRISCHKORN, J. C. De Araújo (org.). **Global Change and Regional Impacts**. Berlin: Springer-V, 2003. p. 87–94.

GAO, L.; KIRBY, M.; AHMAD, M.; MAINUDDIN, M.; BRYAN, B. A. Automatic calibration of a whole-of-basin water accounting model using a comprehensive learning particle swarm optimiser. **Journal of Hydrology**, *[S. l.]*, n. March, p. 124281, 2019. DOI: 10.1016/j.jhydrol.2019.124281. Disponível em: https://doi.org/10.1016/j.jhydrol.2019.124281.

GONDIM, R.; SILVEIRA, C.; DE SOUZA FILHO, F. A.; VASCONCELOS, F.; CID, D. Climate change impacts on water demand and availability using CMIP5 models in the Jaguaribe basin, semi-arid Brazil. **Environmental Earth Sciences**, *[S. l.]*, v. 77, n. 15, p. 1–14, 2018. DOI: 10.1007/s12665-018-7723-9. Disponível em:

http://dx.doi.org/10.1007/s12665-018-7723-9.

GROISMAN, P. Y.; KNIGHT, R. W.; KARL, T. R.; EASTERLING, D. R.; SUN, B.; LAWRIMORE, J. H. Contemporary changes of the hydrological cycle over the contiguous United States: Trends derived from in situ observations. **Journal of Hydrometeorology**, *[S. l.]*, v. 5, n. 1, p. 64–85, 2004. DOI: 10.1175/1525-7541(2004)005<0064:CCOTHC>2.0.CO;2.

GÜNTNER, A.; BRONSTERT, A. Representation of landscape variability and lateral redistribution processes for large-scale hydrological modelling in semi-arid areas. **Journal of Hydrology**, *[S. l.]*, v. 297, n. 1–4, p. 136–161, 2004. DOI: 10.1016/j.jhydrol.2004.04.008.

GUPTA, A.; GOVINDARAJU, R. S. Propagation of structural uncertainty in watershed hydrologic models. **Journal of Hydrology**, *[S. l.]*, v. 575, n. May, p. 66–81, 2019. DOI: 10.1016/j.jhydrol.2019.05.026. Disponível em: https://doi.org/10.1016/j.jhydrol.2019.05.026.

HAMLET, A. F.; MOTE, P. W.; CLARK, M. P.; LETTENMAIER, D. P. Twentieth-century trends in runoff, evapotranspiration, and soil moisture in the western United States. **Journal of Climate**, *[S. l.]*, v. 20, n. 8, p. 1468–1486, 2007. DOI: 10.1175/JCLI4051.1.

HER, Y.; CHAUBEY, I. Impact of the numbers of observations and calibration parameters on equifinality, model performance, and output and parameter uncertainty. **Hydrological Processes**, *[S. l.]*, v. 29, n. 19, p. 4220–4237, 2015. DOI: 10.1002/hyp.10487.

HER, Y.; YOO, S. H.; CHO, J.; HWANG, S.; JEONG, J.; SEONG, C. Uncertainty in hydrological analysis of climate change: multi-parameter vs. multi-GCM ensemble predictions. **Scientific Reports**, *[S. l.]*, v. 9, n. 1, p. 1–22, 2019. DOI: 10.1038/s41598-019-41334-7. Disponível em: http://dx.doi.org/10.1038/s41598-019-41334-7.

HERNANDEZ-SUAREZ, J. S.; NEJADHASHEMI, A. P.; KROPP, I. M.; ABOUALI, M.; ZHANG, Z.; DEB, K. Evaluation of the impacts of hydrologic model calibration methods on predictability of ecologically-relevant hydrologic indices. **Journal of Hydrology**, *[S. l.]*, v. 564, n. January, p. 758–772, 2018. DOI: 10.1016/j.jhydrol.2018.07.056. Disponível em: https://doi.org/10.1016/j.jhydrol.2018.07.056.

IGLESIAS, A.; GARROTE, L. Adaptation strategies for agricultural water management under climate change in Europe. **Agricultural Water Management**, *[S. l.]*, v. 155, p. 113–124, 2015. DOI: 10.1016/j.agwat.2015.03.014. Disponível em: http://dx.doi.org/10.1016/j.agwat.2015.03.014.

INSTITUTO BRASILEIRO DE GEOGRAFIA E ESTATÍSTICA (IBGE). **Diagnóstico Ambiental da Bacia do Rio Jaguaribe.** *[S. l.]*, Salvador, Brazil, 1999.

JAAFAR, H.; AHMAD, F. **GCN250, global curve number datasets for hydrologic modeling and design**, 2019. DOI: https://doi.org/10.6084/m9.figshare.7756202.v1.

JAKEMAN, A. J.; HORNBERGER, G. M. How much complexity is warranted in a rainfall-runoff model? **Water Resources Research**, *[S. l.]*, v. 29, n. 8, p. 2637–2649, 1993. DOI: 10.1029/93WR00877.

KAMALI, B.; MOUSAVI, S. J.; ABBASPOUR, K. C. Automatic calibration of HEC-HMS

using single-objective and multi-objective PSO algorithms. **Hydrological Processes**, *[S. l.]*, v. 27, n. 26, p. 4028–4042, 2013. DOI: 10.1002/hyp.9510.

KENNEDY, J.; EBERHART, R. C. **Swarm Intelligence**. San Francisco: Morgan Kaufmann Publishers, 2001.

KHATTAK, M. S.; BABEL, M. S.; SHARIF, M. Hydro-meteorological trends in the upper Indus River basin in Pakistan. **Climate Research**, *[S. l.]*, v. 46, n. 2, p. 103–119, 2011. DOI: 10.3354/cr00957.

KLEMEŠ, V. Operational testing of hydrological simulation models. **Hydrological Sciences Journal**, *[S. l.]*, v. 31, n. 1, p. 13–24, 1986. DOI: 10.1080/02626668609491024.

KNUTTI, R.; FURRER, R.; TEBALDI, C.; CERMAK, J.; MEEHL, G. A. Challenges in combining projections from multiple climate models. **Journal of Climate**, *[S. l.]*, v. 23, n. 10, p. 2739–2758, 2010. DOI: 10.1175/2009JCLI3361.1.

KUNDZEWICZ, Z. W.; KRYSANOVA, V.; BENESTAD, R. E.; HOV; PINIEWSKI, M.; OTTO, I. M. Uncertainty in climate change impacts on water resources. **Environmental Science and Policy**, *[S. l.]*, v. 79, n. October 2017, p. 1–8, 2018. DOI: 10.1016/j.envsci.2017.10.008. Disponível em: https://doi.org/10.1016/j.envsci.2017.10.008.

KURTZ, W. et al. Integrating hydrological modelling, data assimilation and cloud computing for real-time management of water resources. **Environmental Modelling and Software**, *[S. l.]*, v. 93, p. 418–435, 2017. DOI: 10.1016/j.envsoft.2017.03.011. Disponível em: http://dx.doi.org/10.1016/j.envsoft.2017.03.011.

LAFONTAINE, J. H.; HART, R. M.; HAY, L. E.; FARMER, W. ..; BOCK, A. R.; VIGER, R. J.; MARKSTROM, S. L.; REGAN, R. S.; DRISCOLL, J. M. **Simulation of Water Availability in the Southeastern United States for Historical and Potential Future Climate and Land-Cover Conditions Scientific Investigations Report 2019 – 5039**. Reston, Virginie: [s.n], 2019. DOI: https://doi.org/10.3133/sir20195039. Disponível em: https://pubs.er.usgs.gov/publication/sir20195039.

LEVENE, H. Robust Tests for Equality of Variances. *In*: **In Olkin I, others (eds.), Contributions to Probability and Statistics: Essays in Honor of Harold Hotelling**. Palo Alto: Stanford University Press, 1960.

LI, L. **CAS FGOALS-g3 model output prepared for CMIP6 ScenarioMIP ssp370**Earth System Grid Federation, , 2019. DOI: https://doi.org/10.22033/ESGF/CMIP6.3480.

LIMA NETO, I. E.; WIEGAND, M. C.; CARLOS DE ARAÚJO, J. Redistribution des sédiments due à un réseau dense de réservoirs dans un grand bassin versant semi-aride du Brésil. **Hydrological Sciences Journal**, *[S. l.]*, v. 56, n. 2, p. 319–333, 2011. DOI: 10.1080/02626667.2011.553616.

LIN, F.; CHEN, X.; YAO, H. Evaluating the use of Nash-Sutcliffe efficiency coefficient in goodness-of-fit measures for daily runoff simulation with SWAT. **Journal of Hydrologic Engineering**, *[S. l.]*, v. 22, n. 11, p. 1–9, 2017. DOI: 10.1061/(ASCE)HE.1943-5584.0001580.

LIU, Y. R.; LI, Y. P.; HUANG, G. H.; ZHANG, J. L.; FAN, Y. R. A Bayesian-based multilevel factorial analysis method for analyzing parameter uncertainty of hydrological model. **Journal of Hydrology**, *[S. l.]*, v. 553, p. 750–762, 2017. DOI: 10.1016/j.jhydrol.2017.08.048.

LIU, Yuqiong; GUPTA, Hoshin V. Uncertainty in hydrologic modeling: Toward an integrated data assimilation framework. **Water Resources Research**, *[S. l.]*, v. 43, n. 7, p. 1–18, 2007. DOI: 10.1029/2006WR005756.

LOPES, J. C.; BRAGA, Jr. B. F.; CONEJO, J. L. Simulação Hidrológica: Aplicações de um modelo simplificado. *In*: III SIMPÓSIO BRASILEIRO DE RECURSOS HÍDRICOS 1981, Fortaleza. **Anais** [...]. Fortaleza 1981 p. 42–62.

LUDWIG, R. et al. The role of hydrological model complexity and uncertainty in climate change impact assessment. **Advances in Geosciences**, *[S. l.]*, v. 21, n. August 2009, p. 63–71, 2009. DOI: 10.5194/adgeo-21-63-2009.

MAIER, H. R.; GUILLAUME, J. H. A.; VAN DELDEN, H.; RIDDELL, G. A.; HAASNOOT, M.; KWAKKEL, J. H. An uncertain future, deep uncertainty, scenarios, robustness and adaptation: How do they fit together? **Environmental Modelling and Software**, *[S. l.]*, v. 81, p. 154–164, 2016. DOI: 10.1016/j.envsoft.2016.03.014. Disponível em: http://dx.doi.org/10.1016/j.envsoft.2016.03.014.

MAMEDE, G. L.; ARAÚJO, N. A. M.; SCHNEIDER, C. M.; ARAÚJO, J. C.; HERRMANN, H. J. **Overspill avalanching in a dense reservoir network**. *[S. l.]*, n. below 50, 2012. DOI: 10.1073/pnas.1200398109.

MCMILLAN, Hilary; JACKSON, Bethanna; CLARK, Martyn; KAVETSKI, Dmitri; WOODS, Ross. Rainfall uncertainty in hydrological modelling: An evaluation of multiplicative error models. **Journal of Hydrology**, *[S. l.]*, v. 400, n. 1–2, p. 83–94, 2011. DOI: 10.1016/j.jhydrol.2011.01.026. Disponível em: http://dx.doi.org/10.1016/j.jhydrol.2011.01.026.

MEEHL, G. A.; BOER, G. J.; COVEY, C.; LATIF, Mojib; STOUFFER, R. J. **Coupled Model Intercomparison Project (CMIP)Physical Therapy**, 2000. DOI: 10.1177/017084068800900203. Disponível em: http://web.b.ebscohost.com.ezproxy.fgcu.edu/ehost/pdfviewer/pdfviewer?sid=4fb3a2e8-f118-4461-8790-514e3b326963@sessionmgr114&vid=1&hid=102.

MERZ, R.; BLÖSCHL, G. Regionalisation of catchment model parameters. **Journal of Hydrology**, *[S. l.]*, v. 287, n. 1–4, p. 95–123, 2004. DOI: 10.1016/j.jhydrol.2003.09.028.

MIDDELKOOP, H. et al. Impact of climate change on hydrological regimes and water resources management in the Rhine basin. **Climatic Change**, *[S. l.]*, v. 49, n. 1–2, p. 105–128, 2001. DOI: 10.1023/A:1010784727448.

MILLY, P. C. D.; BETANCOURT, J.; FALKENMARK, M.; HIRSCH, R. M.; KUNDZEWICZ, Z. W.; LETTENMAIER, D. P.; STOUFFER, R. J. Climate change: Stationarity is dead: Whither water management? **Science**, *[S. l.]*, v. 319, n. 5863, p. 573–574, 2008. DOI: 10.1126/science.1151915.

MINVILLE, M.; BRISSETTE, F.; LECONTE, R. Impacts and uncertainty of climate change on water resource management of the Peribonka River System (Canada). **Journal of Water Resources Planning and Management**, *[S. l.]*, v. 136, n. 3, p. 376–385, 2010. DOI: 10.1061/(ASCE)WR.1943-5452.0000041.

MIRANDA, E. E. De. **Brasil em Relevo[dataset]**CampinasEmbrapa Monitoramento por Satélite, , 2005. Disponível em: http://www.relevobr.cnpm.embrapa.br.

MORIASI, D. N.; ARNOLD, J. G.; LIEW, M. W. Van; BINGNER, R. L.; HARMEL, R. D.; VEITH, T. L. Model evaluation guidelines for systematic quantification of accuracy in watershed simulations. **Transactions of the ASABE**, *[S. l.]*, v. 50, n. 3, p. 885–900, 2007.

MURPHY, J. M.; SEXTON, D. M. H.; BARNETT, D. N.; JONES, G. S.; WEBB, M. J.; COLLINS, M.; STAINFORTH, D. A. Quantification of modelling uncertainties in a large ensemble of climate change simulations. **Nature**, *[S. l.]*, v. 430, n. August 2004, p. 768–772, 2004. DOI: 10.1038/nature02770.1.

NDIRITU, J. G.; DANIELL, T. M. An improved genetic algorithm for rainfall-runoff model calibration and function optimization. **Mathematical and Computer Modelling**, *[S. l.]*, v. 33, n. 6–7, p. 695–706, 2001. DOI: 10.1016/S0895-7177(00)00273-9.

O'NEILL, B. C.; KRIEGLER, E.; RIAHI, K.; EBI, K. L.; HALLEGATTE, S.; CARTER, T. R.; MATHUR, R.; VAN VUUREN, D. P. A new scenario framework for climate change research: The concept of shared socioeconomic pathways. **Climatic Change**, *[S. l.]*, v. 122, n. 3, p. 387–400, 2014. DOI: 10.1007/s10584-013-0905-2.

PARKER, W. S. Predicting weather and climate: Uncertainty, ensembles and probability. **Studies in History and Philosophy of Science Part B - Studies in History and Philosophy of Modern Physics**, *[S. l.]*, v. 41, n. 3, p. 263–272, 2010. DOI: 10.1016/j.shpsb.2010.07.006. Disponível em: http://dx.doi.org/10.1016/j.shpsb.2010.07.006.

PETROW, T.; MERZ, B. Trends in flood magnitude, frequency and seasonality in Germany in the period 1951-2002. **Journal of Hydrology**, *[S. l.]*, v. 371, n. 1–4, p. 129–141, 2009. DOI: 10.1016/j.jhydrol.2009.03.024. Disponível em: http://dx.doi.org/10.1016/j.jhydrol.2009.03.024.

PLOUFFE, C. C. F.; ROBERTSON, C.; CHANDRAPALA, L. Comparing interpolation techniques for monthly rainfall mapping using multiple evaluation criteria and auxiliary data sources: A case study of Sri Lanka. **Environmental Modelling and Software**, *[S. l.]*, v. 67, p. 57–71, 2015. DOI: 10.1016/j.envsoft.2015.01.011. Disponível em: http://dx.doi.org/10.1016/j.envsoft.2015.01.011.

POFF, N. L. et al. Sustainable water management under future uncertainty with eco-engineering decision scaling. **Nature Climate Change**, *[S. l.]*, v. 6, n. 1, p. 25–34, 2016. DOI: 10.1038/nclimate2765.

PONCELET, C.; MERZ, R.; MERZ, B.; PARAJKA, J.; OUDIN, L.; ANDRÉASSIAN, V.; PERRIN, C. Process-based interpretation of conceptual hydrological model performance using a multinational catchment set. **Water Resources Research**, *[S. l.]*, v. 53, n. 8, p. 7247–7268, 2017. DOI: 10.1002/2016WR019991.

RAJE, D.; KRISHNAN, R. Bayesian parameter uncertainty modeling in a macroscale hydrologic model and its impact on Indian river basin hydrology under climate change. **Water Resources Research**, *[S. l.]*, v. 48, n. 8, p. 1–17, 2012. DOI: 10.1029/2011WR011123.

RIVAS-TABARES, D.; TARQUIS, A. M.; WILLAARTS, B.; DE MIGUEL, A. An accurate evaluation of water availability in sub-arid Mediterranean watersheds through SWAT: Cega-Eresma-Adaja. **Agricultural Water Management**, *[S. l.]*, v. 212, n. January 2018, p. 211–225, 2019. DOI: 10.1016/j.agwat.2018.09.012. Disponível em: https://doi.org/10.1016/j.agwat.2018.09.012.

ROOD, S. B.; PAN, J.; GILL, K. M.; FRANKS, C. G.; SAMUELSON, G. M.; SHEPHERD, A. Declining summer flows of Rocky Mountain rivers: Changing seasonal hydrology and probable impacts on floodplain forests. **Journal of Hydrology**, *[S. l.]*, v. 349, n. 3–4, p. 397–410, 2008. DOI: 10.1016/j.jhydrol.2007.11.012.

RWASOKA, D. T.; MADAMOMBE, C. E.; GUMINDOGA, W.; KABOBAH, A. T. Calibration, validation, parameter indentifiability and uncertainty analysis of a 2 - parameter parsimonious monthly rainfall-runoff model in two catchments in Zimbabwe. **Physics and Chemistry of the Earth**, *[S. l.]*, v. 67–69, p. 36–46, 2014. DOI: 10.1016/j.pce.2013.09.015. Disponível em: http://dx.doi.org/10.1016/j.pce.2013.09.015.

SALVI, K.; KANNAN, S.; GHOSH, S. Statistical downscaling and bias-correction for projections of Indian rainfall and temperature in climate change studies. In: INTERNATIONAL CONFERENCE ON ENVIRONMENTAL AND COMPUTER SCIENCE, 4, 2011, Singapore. **Proceedings**.... Singapore: IPCBEE, 2011, p. 7–11. Disponível em: http://www.ipcbee.com/vol19/2-ICECS2011R00006.pdf.

SAMUEL, J.; COULIBALY, P.; METCALFE, R. A. Estimation of continuous streamflow in ontario ungauged basins: Comparison of regionalization methods. **Journal of Hydrologic Engineering**, *[S. l.]*, v. 16, n. 5, p. 447–459, 2011. DOI: 10.1061/(ASCE)HE.1943-5584.0000338.

SEZEN, C.; BEZAK, N.; BAI, Y.; ŠRAJ, M. Hydrological modelling of karst catchment using lumped conceptual and data mining models. **Journal of Hydrology**, *[S. l.]*, v. 576, n. December 2018, p. 98–110, 2019. DOI: 10.1016/j.jhydrol.2019.06.036.

SHAFII, M.; TOLSON, B.; MATOTT, L. S. Uncertainty-based multi-criteria calibration of rainfall-runoff models: A comparative study. **Stochastic Environmental Research and Risk Assessment**, *[S. l.]*, v. 28, n. 6, p. 1493–1510, 2014. DOI: 10.1007/s00477-014-0855-x.

SHAHED BEHROUZ, M; ZHU, Z; MATOTT, L. S; RABIDEAU, A J. A new tool for automatic calibration of the Storm Water Management Model (SWMM). **Journal of Hydrology**, *[S. l.]*, v. 581, p. 124436, 2020. DOI: 10.1016/j.jhydrol.2019.124436. Disponível em: https://doi.org/10.1016/j.jhydrol.2019.124436.

SHARMA, D.; BABEL, M. S. Assessing hydrological impacts of climate change using bias-corrected downscaled precipitation in Mae Klong basin of Thailand. **Meteorological Applications**, *[S. l.]*, v. 25, n. 3, p. 384–393, 2018. DOI: 10.1002/met.1706.

SILVEIRA, C. S.; SOUZA FILHO, F. A.; VASCONCELOS JÚNIOR, F. C. Streamflow

projections for the Brazilian hydropower sector from RCP scenarios. **Journal of Water and Climate Change**, *[S. l.]*, v. 8, n. 1, p. 114–126, 2017. DOI: 10.2166/wcc.2016.052.

SIVAPALAN, M. et al. IAHS Decade on Predictions in Ungauged Basins (PUB), 2003-2012: Shaping an exciting future for the hydrological sciences. **Hydrological Sciences Journal**, *[S. l.]*, v. 48, n. 6, p. 857–880, 2003. DOI: 10.1623/hysj.48.6.857.51421.

SMITH, De Ralph C. **Uncertainty quantification: theory, implementation, and applications.** [s.l.] : Siam, 2014.

SORDO-WARD, A.; GRANADOS, I.; MARTÍN-CARRASCO, F.; GARROTE, L. Impact of Hydrological Uncertainty on Water Management Decisions. **Water Resources Management**, *[S. l.]*, v. 30, n. 14, p. 5535–5551, 2016. DOI: 10.1007/s11269-016-1505-5. Disponível em: http://dx.doi.org/10.1007/s11269-016-1505-5.

SOUZA FILHO, F. A. de. **Projeto Ceará 2050: Diagnóstico dos Recursos Hídricos no Ceará**. Fortaleza: [s.n], 2018. Disponível em: http://www.ceara2050.ce.gov.br/api/wp-content/uploads/2018/10/ceara-2050-estudo-setorial-especial-recursos-hidricos.pdf.

SOUZA FILHO, F. A.; LALL, U. **Seasonal to interannual ensemble streamflow forecasts for Ceara , Brazil : Applications of a multivariate , semiparametric algorithm.** *[S. l.]*, v. 39, n. 11, p. 1–13, 2003. DOI: 10.1029/2002WR001373.

SUPERINTENDÊNCIA DE DESENVOLVIMENTO DO NORDESTE (SUDENE). **Plano de Aproveitamento Integrado de Recursos Hídricos do Nordeste do Brasil** *[S.I.]* Recife, Brazil, 1980.

SWART, N. C. ET AL. SWART, N C; COLE, J. N.S.; KHARIN, V. V.; LAZARE, M; SCINOCCA, J F.; GILLETT, N P.; ANSTEY, J; ARORA, VIVEK; CHRISTIAN, JAMES R.; et al.**CCCma CanESM5 model output prepared for CMIP6 ScenarioMIP ssp126** Earth System Grid Federation, , 2019. DOI: doi.org/10.22033/ESGF/CMIP6.3683.

TATEBE, H.; WATANABE, M. **MIROC MIROC6 model output prepared for CMIP6 CMIP historical**Earth System Grid Federation, , 2018. DOI: https://doi.org/10.22033/ESGF/CMIP6.5603.

TRINH, T.; JANG, S.; ISHIDA, K.; OHARA, N.; CHEN, Z. Q.; ANDERSON, M. L.; DARAMA, Y.; CHEN, J.; KAVVAS, M. L. Reconstruction of historical inflows into and water supply from shasta dam by coupling physically based hydroclimate model with reservoir operation model. **Journal of Hydrologic Engineering**, *[S. l.]*, v. 21, n. 9, p. 1–12, 2016. DOI: 10.1061/(ASCE)HE.1943-5584.0001391.

TUNG, Y. K. Effect of uncertainties on probabilistic-based design capacity of hydrosystems. **Journal of Hydrology**, *[S. l.]*, v. 557, p. 851–867, 2018. DOI: 10.1016/j.jhydrol.2017.12.059. Disponível em: https://doi.org/10.1016/j.jhydrol.2017.12.059.

ULIANA, E. M.; DE ALMEIDA, F. T.; DE SOUZA, A. P.; DA CRUZ, I. F.; LISBOA, L.; DE SOUSA JÚNIOR, M. F. Application of SAC-SMA and IPH II hydrological models in the teles pires river basin, Brazil. **Revista Brasileira de Recursos Hidricos**, *[S. l.]*, v. 24, 2019. DOI: 10.1590/2318-0331.241920180082.

VALLAM, P.; QIN, X. S.; YU, J. J. Uncertainty Quantification of Hydrologic Model. **APCBEE Procedia**, *[S. l.]*, v. 10, p. 219–223, 2014. DOI: 10.1016/j.apcbee.2014.10.042.

VANSTEENKISTE, T.; TAVAKOLI, M.; VAN STEENBERGEN, N.; DE SMEDT, F.; BATELAAN, O.; PEREIRA, F.; WILLEMS, P. Intercomparison of five lumped and distributed models for catchment runoff and extreme flow simulation. **Journal of Hydrology**, *[S. l.]*, v. 511, p. 335–349, 2014. DOI: 10.1016/j.jhydrol.2014.01.050. Disponível em: http://dx.doi.org/10.1016/j.jhydrol.2014.01.050.

VETTER, T. et al. Evaluation of sources of uncertainty in projected hydrological changes under climate change in 12 large-scale river basins. **Climatic Change**, *[S. l.]*, v. 141, n. 3, p. 419–433, 2017. DOI: 10.1007/s10584-016-1794-y.

VIVIROLI, D.; MITTELBACH, H.; GURTZ, J.; WEINGARTNER, R. Continuous simulation for flood estimation in ungauged mesoscale catchments of Switzerland - Part II: Parameter regionalisation and flood estimation results. **Journal of Hydrology**, *[S. l.]*, v. 377, n. 1–2, p. 208–225, 2009. DOI: 10.1016/j.jhydrol.2009.08.022. Disponível em: http://dx.doi.org/10.1016/j.jhydrol.2009.08.022.

VON STORCH, J. et al. **MPI-M MPI-ESM1.2-HR model output prepared for CMIP6 HighResMIP highresSST-present**Earth System Grid Federation, , 2017. DOI: https://doi.org/10.22033/ESGF/CMIP6.6584.

VRUGT, J. A. Markov chain Monte Carlo simulation using the DREAM software package: Theory, concepts, and MATLAB implementation. **Environmental Modelling and Software**, *[S. l.]*, v. 75, p. 273–316, 2016. DOI: 10.1016/j.envsoft.2015.08.013. Disponível em: http://dx.doi.org/10.1016/j.envsoft.2015.08.013.

VRUGT, J. A.; GUPTA, H. V.; BASTIDAS, L. A.; BOUTEN, W.; SOROOSHIAN, S. Effective and efficient algorithm for multiobjective optimization of hydrologic models. **Water Resources Research**, *[S. l.]*, v. 39, n. 8, p. 1–19, 2003. DOI: 10.1029/2002WR001746.

VRUGT, J. A.; TER BRAAK, C. J. F.; CLARK, M. P.; HYMAN, J. M.; ROBINSON, B. A. Treatment of input uncertainty in hydrologic modeling: Doing hydrology backward with Markov chain Monte Carlo simulation. **Water Resources Research**, *[S. l.]*, v. 44, n. 12, p. 1–15, 2008. DOI: 10.1029/2007wr006720.

VRUGT, J. A.; TER BRAAK, C. J. F.; GUPTA, H. V.; ROBINSON, B. A. Equifinality of formal (DREAM) and informal (GLUE) Bayesian approaches in hydrologic modeling? **Stochastic Environmental Research and Risk Assessment**, *[S. l.]*, v. 23, n. 7, p. 1011–1026, 2009. DOI: 10.1007/s00477-008-0274-y.

WAGENER, T.; MONTANARI, A. Convergence of approaches toward reducing uncertainty in predictions in ungauged basins. **Water Resources Research**, *[S. l.]*, v. 47, n. 6, p. 1–8, 2011. DOI: 10.1029/2010WR009469.

WALLNER, M.; HABERLANDT, U.; DIETRICH, J. A one-step similarity approach for the regionalization of hydrological model parameters based on self-organizing maps. **Journal of Hydrology**, *[S. l.]*, v. 494, p. 59–71, 2013. DOI: 10.1016/j.jhydrol.2013.04.022. Disponível em: http://dx.doi.org/10.1016/j.jhydrol.2013.04.022.

WIDÉN-NILSSON, E.; HALLDIN, S.; XU, C. Y. Global water-balance modelling with WASMOD-M: Parameter estimation and regionalisation. **Journal of Hydrology**, *[S. l.]*, v. 340, n. 1–2, p. 105–118, 2007. DOI: 10.1016/j.jhydrol.2007.04.002.

WU, T. et al. **BCC BCC-CSM2MR model output prepared for CMIP6 CMIP 1pctCO2**Earth System Grid Federation, , 2018. DOI: https://doi.org/10.22033/ESGF/CMIP6.2833.

XAVIER, Alexandre C.; KING, Carey W.; SCANLON, Bridget R. Daily gridded meteorological variables in Brazil (1980–2013). **International Journal of Climatology**, *[S. l.]*, v. 36, n. 6, p. 2644–2659, 2016. DOI: 10.1002/joc.4518.

YUKIMOTO, S. et al. **MRI MRI-ESM2.0 model output prepared for CMIP6 CFMIP amip-p4K-lwoff**Earth System Grid Federation, , 2019. DOI: https://doi.org/10.22033/ESGF/CMIP6.6772.

ZAKERMOSHFEGH, M.; NEYSHABOURI, S. A. A. S.; LUCAS, C. Automatic calibration of lumped conceptual rainfall-runoff model using Particle Swarm Optimization. **Journal of Applied Sciences**, *[S. l.]*, v. 8, n. 20, p. 3703–3708, 2008.